Circulation Research

ORIGINAL RESEARCH

# cDC1s Promote Atherosclerosis via Local Immunity and Are Targetable for Therapy

Miguel Galán, Laura Fernández-Méndez, Vanessa Núñez, Marcos Femenía-Muiña, Pau Figuera-Belmonte, Elena Moya-Ruiz, Sarai Martínez-Cano, Elena Hernández-García, Manuel Rodrigo-Tapias, Ana Rodríguez-Ronchel, Carlos Relaño-Rupérez, Stefanie K. Wculek, Alberto Benguria, Ana Dopazo, Sandrine Henri, Suin Jo, Tian-Tian Liu, Bernard Malissen, Kenneth M. Murphy, Almudena R. Ramiro, Susana Carregal-Romero, Jesús Ruiz-Cabello, Iñaki Robles-Vera, David Sancho

**BACKGROUND:** Atherosclerosis is characterized by immune cell accumulation in the arterial wall and adaptive CD4$^+$ Th1 immunity contributes to atherosclerosis development. However, how conventional dendritic cells (cDCs) orchestrate this adaptive response remains controversial. This study unveils strategies for the gain and loss of function of cDCs to decipher their role in atherosclerosis induction in relation to adaptive T-cell immunity.

**METHODS:** We tested atherosclerosis in *Ldlr*$^{-/-}$ mice fed a high-cholesterol diet (HCD). Expansion of cDCs in vivo was achieved by overexpression of FLT3L (Fms-like tyrosine kinase 3 ligand), while the effect of ablation of conventional type 1 dendritic cells (cDC1s) in atherosclerosis was analyzed by grafting bone marrow from different mouse models of cDC1 depletion, including *Xcr1*$^{Cre–DTA}$ and *Irf8*Δ32 mice, into lethally irradiated *Ldlr*$^{-/-}$ recipients before HCD. CD3$^+$ T-cell subsets were analyzed using flow cytometry or scRNA-seq. Nanoparticles loaded with dexamethasone and decorated with anti-CLEC9A antibody to target cDC1s were tested for immunotherapy.

**RESULTS:** Expansion of dendritic cells in *Ldlr*$^{-/-}$ mice fed HCD for 8 weeks led to increased atherosclerotic lesion, which was prevented when *Ldlr*$^{-/-}$ mice were grafted before dendritic cell expansion with *Xcr1*$^{Cre–DTA}$ cDC1-depleted bone marrow compared with controls. Consistently, even in the absence of dendritic cell expansion, cDC1 deficiency prevented HCD-induced atherosclerosis. The scRNA-seq analysis of aortic CD3$^+$ T cells in this experimental approach showed a local reduction in CD4$^+$ Th1 and CD8$^+$ IFN (interferon)-γ$^+$ T cells in the absence of cDC1s compared with control mice. Mechanistically, stimulator of IFN genes in cDC1s was required for the proatherogenic function of cDC1s. As a potential cDC1-targeted immunotherapy for atherosclerosis, we generated lipid nanoparticles decorated with an anti-CLEC9A antibody to specifically target cDC1s. When loaded with the immunosuppressive drug dexamethasone, these nanoparticles promoted a reduction of the atherosclerotic lesion in *Ldlr*$^{-/-}$ mice fed HCD, correlating with decreased CD4$^+$ Th1 and CD8$^+$ IFN-γ$^+$ T cells in the spleen. These immunosuppressive nanoparticles, however, did not impair antiviral response.

**CONCLUSIONS:** Using state-of-the-art strategies, our results establish that cDC1s have a proatherogenic role in atherosclerosis by boosting CD4$^+$ and CD8$^+$ T-cell immunity and propose that cDC1s can be targeted with an immunosuppressive drug to decrease atherosclerosis progression.

**GRAPHIC ABSTRACT:** A graphic abstract is available for this article.

**Key Words:** atherosclerosis ■ dendritic cells ■ immunotherapy ■ mice ■ nanoparticles





Atherosclerosis is a systemic inflammatory disease characterized by lipid accumulation and immune cell infiltration in the arterial walls leading to the formation of atheroma plaques.[1] Although atherosclerosis is the leading cause of cardiovascular diseases and the contribution of adaptive immunity is well studied,

Correspondence to: David Sancho, Centro Nacional de Investigaciones Cardiovasculares Carlos III (CNIC), Madrid, Spain. Email dsancho@cnic.es
Supplemental Material is available at https://www.ahajournals.org/doi/suppl/10.1161/CIRCRESAHA.124.325792.
For Sources of Funding and Disclosures, see page XXX.

*Circulation Research* is available at www.ahajournals.org/journal/res

ORIGINAL RESEARCH

## Novelty and Significance

### What Is Known?

- Conventional dendritic cells are professional antigen-presenting cells that orchestrate innate and adaptive immunity.
- There is growing evidence for the importance of adaptive immunity in atherosclerosis and particularly, the function of dendritic cells in priming distinct T-cell responses. However, the precise function of conventional type 1 dendritic cells (cDC1s) in atherosclerosis is controversial.

### What New Information Does This Article Contribute?

- After previous controversial results, we used more refined strategies for expansion (gain of function) or depletion (loss of function) of cDC1s to establish their proatherogenic role in inducing a local aortic CD4$^+$ Th1 and CD8$^+$ IFN (interferon)-γ$^+$ effector response.
- Activation of cDC1s in the plaque involves the stimulator of interferon genes pathway.
- Lipid nanoparticles loaded with the immunosuppressive drug dexamethasone are a potential immunotherapy for atherosclerosis that specifically targets cDC1s through the cDC1-specific receptor CLEC9A.

Previous reports suggest contradictory roles for cDC1s in atherosclerosis development, suggesting either protective or detrimental effects, whereas other reports show no effect on atherosclerosis progression on cDC1 depletion. Using different gain and loss of function approaches, we demonstrate that cDC1s contribute to CD3$^+$ T-cell immunity in atherosclerosis. In vivo expansion of dendritic cells in *Ldlr*$^{-/-}$ mice fed high-cholesterol diet for 8 weeks led to increased atherosclerotic lesion, which was dependent on cDC1s, because it was prevented when *Ldlr* $^{-/-}$ mice were grafted before dendritic cell expansion with Xcr1$^{Cre–DTA}$ cDC1-depleted BM compared with controls. The scRNA-seq analysis of aortic CD3$^+$ T cells showed a local reduction in CD4$^+$ Th1 and CD8$^+$ IFN-γ$^+$ T cells in the absence of cDC1s compared with control mice. Mechanistically, we demonstrate that stimulator of interferon gene activation in cDC1s contributes to the proatherogenic effect. Based on the proatherogenic function of cDC1s, we developed a novel immunotherapy for atherosclerosis based on cDC1-targeted lipid nanoparticles loaded with the immunosuppressive drug dexamethasone. These nanoparticles prevented progression of the atherosclerotic lesion in *Ldlr*$^{-/-}$ mice fed a high-cholesterol diet, which correlated with decreased CD4$^+$ Th1 and CD8$^+$ IFN-γ$^+$ T cells in the spleen.

## Nonstandard Abbreviations and Acronyms

| | |
|---|---|
| **BM** | bone marrow |
| **cDC1s** | conventional type 1 dendritic cells |
| **cDC2s** | conventional type 2 dendritic cells |
| **cDCs** | conventional dendritic cells |
| **CTR** | |
| **DCs** | dendritic cells |
| | empty pUMVC3 vector |
| **FLT3L** | Fms-like tyrosine kinase 3 ligand |
| **HCD** | High-cholesterol diet |
| **HDL** | high-density lipoprotein |
| **IFN** | interferon |
| **IL** | interleukin |
| **IRF8** | interferon regulatory factor 8 |
| **LDL** | low-density lipoprotein |
| **mFLex** | mammalian expression vector expressing a secreted form of mouse FLT3L |
| **STING** | Stimulator of interferon genes |
| **TCR** | T-cell receptor |
| **TLR** | toll-like receptor 3 |

the knowledge of how the adaptive immune response can be manipulated for immunotherapy is still limited.[2–4] Conventional dendritic cells (cDCs) are professional antigen-presenting cells that orchestrate innate and adaptive immunity and are divided into 2 main lineages. conventional type 1 dendritic cells (cDC1s) and conventional type 2 dendritic cells (cDC2s) both derive from a common dendritic cell (DC) progenitor.[5] FLT3L (fms-like tyrosine kinase 3 ligand) promotes the differentiation of these precursors into fully functional DCs.[6] Mice lacking FLT3L or FLT3 (CD135) genes show a drastic reduction in DC populations,[7,8] whereas injection of exogenous FLT3L in mice increases the frequency of DCs subsets.[9] cDC1s from mice require the transcription factors ID2, BATF3, IRF8 (interferon regulatory factor 8) and NFIL3 for their development[10] and are characterized by expression of XCR1 and CLEC9A.[11–13] cDC1s are highly efficient in presenting exogenous antigen on MHC class I molecules to CD8$^+$ T cells, a process called cross-presentation.[14,15] cDC1s also promote CD4$^+$ Th1 responses by providing IL (interleukin)-12 during priming.[16,17] On the other hand, murine cDC2s rely on IRF4, NOTCH2, KLF4, and ZEB2 transcription factors[10,18] and express CD11b and SIRPa.[19] cDC2s are highly efficient at presenting antigens on MHC

class II molecules to CD4+ T helper cells, priming Th2 and Th17 responses.[20,21]

Despite growing evidence for the important role of adaptive immunity in atherosclerosis and the key function of DCs in priming distinct CD3+ T-cell responses, the precise function of cDC1s in atherosclerosis is controversial. Initial results suggested an atheroprotective role for cDC1s because *Ldlr*$^{-/-}$ *Flt3*$^{-/-}$ mice showed a deficiency in aortic cDC1s and a concomitant decrease in CD4+ Foxp3+ Tregs, with exacerbated atherosclerotic lesions.[22] Conversely, other reports have shown that cDC1 depletion is associated with reduced atherosclerosis. For instance, mice with a specific deletion of IRF8 in CD11c+ cells exhibited reduced infiltration of cDC1s in the aorta, correlating with lower CD3+ T-cell infiltration and smaller atherosclerotic lesions.[23] Furthermore, bone marrow (BM) restricted deletion of CLEC9A, a receptor specific to cDC1s involved in cross-presentation,[12] in atheroprone *Ldlr*$^{-/-}$ mice also reduced atherosclerosis by increasing an anti-inflammatory IL-10–mediated response.[24] Similarly, the absence of BATF3, which compromised cDC1 presence and function,[25] in *ApoE*$^{-/-}$ mice resulted in fewer cDC1s in the aorta, and diminished CD4+ Th1 polarization, leading to decreased atherosclerosis pathology.[26] However, other reports using a similar strategy to impair cDC1s by targeting BATF3 did not find any impact on atherosclerosis. In one study, *Ldlr*$^{-/-}$ *Batf3*$^{-/-}$ mice fed with high-cholesterol diet (HCD) did not show differences in atherosclerosis development.[27] Similarly, another study showed that *Ldlr*$^{-/-}$ mice grafted with *Batf3*$^{-/-}$ BM had fewer cDC1s and reduced cross-priming capacity but developed similar atherosclerotic lesions on HCD compared with mice grafted with wild-type BM.[28] These reports suggest a complex role for cDC1s in atherosclerosis that requires novel strategies to establish their function.

In addition, cDC1-directed immunotherapy has not been fully developed yet. To target pharmacological entities to cDC1s in a flexible manner, one option is the use of lipid-based nanoparticles. Liposomes exhibit a high capacity to solubilize and stabilize a wide range of drugs and act as carriers to improve delivery to the specific target cell type. Liposomal drug formulations, such as Doxil, are clinically approved[29,30] and nanoparticles have emerged as promising tools in the diagnosis and treatment of atherosclerosis.[31] For instance, nanoparticles coated with ligands that recognize and bind to receptors expressed on macrophages ensure precise drug delivery.[32] However, nanoparticles targeted to cDC1s have not been developed as an immunotherapy for atherosclerosis.

Here, we explore new combined gain and loss of function strategies to dissect the role of cDC1s in atherosclerosis. Furthermore, we generated a novel preclinical atherosclerosis immunotherapy based on the specific targeting of cDC1s with nanoparticles loaded with an anti-inflammatory drug dexamethasone.

# METHODS

## Data Availability

The data that support the findings of this study are available from the corresponding author upon reasonable request. A detailed methods section is available in the Supplemental Material I. A list of all the reagents and their references is available in Table S1 in detailed methods. For more information about the reagents, please see the Major Resources Table in Supplemental Material II.

# RESULTS

## Expansion of cDC1s Promotes Atherosclerosis

To analyze the effect of DC expansion in early atherosclerosis, we hydrodynamically injected a plasmid encoding for the secreted extracellular domain of mouse FLT3L (mFLex [mammalian expression vector expressing a secreted form of mouse FLT3L]), which largely expands DCs,[33] or empty pUMVC3 vector (CTR) in 8-week-old *Ldlr*$^{-/-}$ male mice. Then, the animals were subsequently fed with HCD for 8 weeks (Figure 1A). Hydrodynamic injection of mFLex mainly expands cDC1s (8.8-fold expansion) and plasmacytoid DCs (5.5-fold expansion), whereas other immune cells are also expanded in a lower ratio (1–2.5-fold expansion; Figure S1A). Analysis of total DCs, cDC1s, and cDC2s confirmed the expansion of both cDC subsets in the spleen and aorta of mFLex-injected *Ldlr*$^{-/-}$ mice compared with empty CTR vector-injected *Ldlr*$^{-/-}$ mice at the end point (Figure S1B). Expansion of DCs in *Ldlr*$^{-/-}$ mice fed HCD did not affect body weight gain or lipid profile (LDL [low-density lipoprotein], HDL [high-density lipoprotein], total cholesterol, and free cholesterol; Figure 1B and 1C). However, expansion of DCs induced an increase in Oil Red-O+ atherosclerotic lesion size in both the aorta and the aortic heart valve (Figure 1D), correlating with increased CD3+ T-cell number per area of lesion (Figure 1E). Other plaque parameters tested, such as collagen staining, necrotic core, MAC2 (macrophage) staining, and caspase 3 were similar between groups (Figure S1C).

We also explored the effect of DC expansion in already established atherosclerosis by mFLex (or CTR vector) hydrodynamic injection in *Ldlr*$^{-/-}$ male mice already fed HCD for 8 weeks. After the injection, *Ldlr*$^{-/-}$ mice were fed HCD for a further 4 weeks (Figure S2A). Although body weight gain was not affected (Figure S2B), late DC expansion resulted in increased atherosclerotic lesion in the aorta and the aortic heart valve (Figure S2C).

These results could suggest that DC expansion could have a proatherogenic role. However, because of the expansion of other immune cells apart from cDC1s

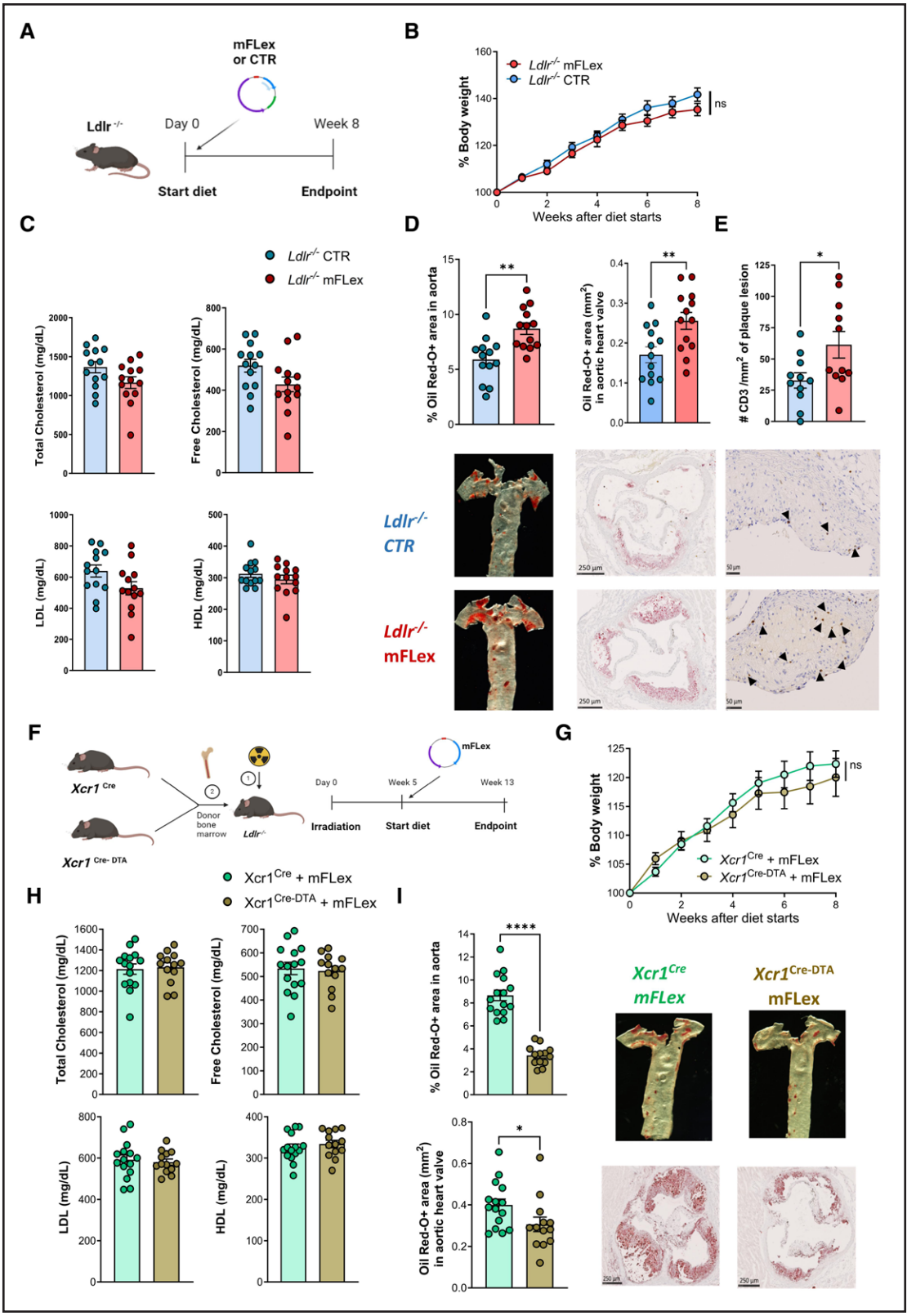


**Figure 1. Expansion of conventional type 1 dendritic cells (cDC1s) increases atherosclerosis lesion independently of lipid profile.**

**A**, Expansion of DCs at early stage of atherosclerosis. *Ldlr*$^{-/-}$ male mice were intravenously injected with mFLex (mammalian expression vector expressing a secreted form of mouse Fms-like tyrosine kinase 3 ligand) or control plasmid (CTR) and fed high-cholesterol diet (HCD) for 8 weeks, followed by euthanasia and analysis. **B**, Percentage of body weight tracked for 8 weeks of HCD after DCs expansion (n=13/group). **C**, Total cholesterol, free cholesterol, LDL (low-density lipoprotein), and HDL (high-density lipoprotein) analysis in plasma at end (*Continued*)

with mFLex injection (Figure S1A), we cannot attribute the increased atherosclerosis lesion to cDC1s. To dissect the specific contribution of cDC1s to atherogenesis induced on hydrodynamic injection with mFLex, we tested the effect of mFLex hydrodynamic injection in mice lacking cDC1s. To this aim, lethally irradiated *Ldlr*$^{-/-}$ CD45.1 male mice were grafted with BM from *Xcr1*$^{Cre–DTA}$ mice (*Xcr1*$^{Cre}$ x lox-STOP-lox DTA, resulting in DTA expression under *Xcr1* driver and leading to cDC1 impairment) or with BM from control *Xcr1*$^{Cre}$ mice. After BM reconstitution (Figure S2D), *Ldlr*$^{-/-}$ CD45.1 mice received a hydrodynamic injection of mFLex plasmid and were fed HCD for 8 weeks (Figure 1F). Comparing the effect of mFLex in immune cell subsets, *Xcr1*$^{Cre–DTA}$ mice fully depleted cDC1s, along with a reduction in T cells that could be a consequence of cDC1 reduction (Figure S2E), but the rest of the immune cells were similarly affected by mFLex. At the end point, we confirmed that both cDC1s and cDC2s were expanded in the spleen of *Ldlr*$^{-/-}$ grafted with control *Xcr1*$^{Cre}$ BM and cDC2s but not cDC1s were expanded in *Ldlr*$^{-/-}$ grafted with *Xcr1*$^{Cre–DTA}$ BM (Figure S2F). Depletion of cDC1s on mFLex DC expansion did not affect body weight gain or lipid profile (Figure 1G and 1H) but led to a decrease in atherosclerotic lesions in the aorta and in the aortic heart valve (Figure 1I). Taking together all these results, hydrodynamic injection of mFLex increases atherosclerosis disease in a cDC1-dependent fashion.

## cDC1 Impairment Reduces Atheroma Plaque Formation

To explore whether the impairment of cDC1s could also affect atherosclerosis development in a homeostatic setting, without mFLex injection, lethally irradiated *Ldlr*$^{-/-}$ CD45.1 male mice were grafted with *Xcr1*$^{Cre–DTA}$ or control *Xcr1*$^{Cre}$ BM. After BM reconstitution (Figure S3A) mice were fed HCD for 8 weeks (Figure 2A). *Xcr1*$^{Cre–DTA}$ grafted *Ldlr*$^{-/-}$ mice showed a reduction in the number of cDC1s both in the aorta and the spleen compared with *Xcr1*$^{Cre}$ grafted *Ldlr*$^{-/-}$ mice (Figure 2B) Decreased cDC1 numbers did not affect body weight gain (Figure S3B) or cholesterol concentrations (Figure 2C) but associated with a decreased atherosclerotic lesion in aorta and aortic heart valves (Figure 2D). Flow cytometry analysis of aorta at end point showed a reduction in CD3$^{+}$ T cells, but not in B cells, monocytes, neutrophils, or NK cells in *Xcr1*$^{Cre–DTA}$ grafted *Ldlr*$^{-/-}$ compared with control (Figure S3C). At systemic level, no difference in any immune population was observed in the spleen at end point (Figure S3C). In addition, analysis of aortic plaque lesions showed that *Ldlr*$^{-/-}$ mice grafted with *Xcr1*$^{Cre–DTA}$ BM and fed HCD had a lower number of CD3$^{+}$ T cells infiltrating into the atherosclerotic lesion compared with *Ldlr*$^{-/-}$ mice grafted with control *Xcr1*$^{Cre}$ BM (Figure 2E). However, no differences in collagen deposition, necrotic core, macrophage infiltration, or caspase 3$^{+}$ cells in the lesion were observed (Figure S3D). These results suggest that cDC1s promote atherosclerosis.

We also analyzed the proatherogenic role of cDC1s in *Ldlr*$^{-/-}$ female mice after the same experimental approach: *Ldlr*$^{-/-}$ CD45.1 female mice were grafted with *Xcr1*$^{Cre–DTA}$ or control *Xcr1*$^{Cre}$ BM. After BM reconstitution, mice were fed HCD for 8 weeks (Figure S4A and S4B). *Xcr1*$^{Cre–DTA}$ grafted *Ldlr*$^{-/-}$ mice showed a drastic reduction in number of cDC1s and a mild compensatory increase of cDC2s in the spleen compared with control *Xcr1*$^{Cre}$ grafted *Ldlr*$^{-/-}$ mice (Figure S4C). Similar to males, decreased cDC1 numbers did not affect body weight gain (Figure S4D) or cholesterol concentrations (Figure S4E) but were associated with a reduction of atherosclerotic lesions in aorta (Figure S4F).

To validate that cDC1s promote atherosclerosis with an independent approach, we used a different mouse model to deplete cDC1s by targeting IRF8, which is required for cDC1 differentiation. A 421bp deletion of an enhancer located 32-kb downstream of the Irf8 transcriptional start site (+32-kb Irf8) using CRISPR/Cas9 endonuclease results in the elimination of all cDC1s.[34] BM from *Irf8*Δ32 mice or wild type as a control were transferred to lethally irradiated *Ldlr*$^{-/-}$ CD45.1 male mice (Figure 3A; Figure S5A). At the end point, we observed a complete depletion of cDC1s and a compensatory increase of cDC2s in the spleen (Figure 3B). Analysis of other immune cells of the aorta and spleen by flow cytometry showed a mild reduction in CD3$^{+}$ T cells in the spleen, but not in B cells, monocytes, neutrophils, or NK cells in the spleen or aorta from *Xcr1*$^{Cre–DTA}$ grafted *Ldlr*$^{-/-}$ compared with control (Figure S5B). Depletion of cDC1s did not affect body weight gain (Figure S5C) or lipid

**Figure 1 Continued.** point (n=13/group). **D**, Quantification (**top**) and representative images of the mean (**bottom**) of atherosclerotic lesion by Oil Red-O staining of the aorta (**left**) or aortic heart valve (**right**; n=13/group). **E**, Staining of CD3$^{+}$ T cells infiltrating the aortic heart valve lesion showing quantification (**top**) and representative images of the mean (**bottom**; n=11/group). **F**, *Ldlr*$^{-/-}$ CD45.1 male mice were grafted with bone marrow (BM) from *Xcr1*$^{Cre}$ or *Xcr1*$^{Cre–DTA}$ donor mice. After BM reconstitution, DCs were expanded by intravenous injection of mFLex plasmid and mice were fed HCD for 8 weeks, followed by euthanasia and analysis. **G**, Percentage of body weight tracked for 8 weeks of HCD after DCs expansion (n=15 in *Xcr1*$^{Cre–}$ +mFLex and n=13 in *Xcr1*$^{Cre–DTA}$ + mFLex groups). **H**, Total cholesterol, free cholesterol, LDL, and HDL analysis in plasma at end point (n=15 in *Xcr1*$^{Cre–}$ + mFLex and n=13 in *Xcr1*$^{Cre–DTA}$ + mFLex group). **I**, Quantification (**left**) and representative images of the mean (**right**) of atherosclerotic lesion by Oil Red-O staining of the aorta (**top**) or aortic heart valve (**bottom**; n=15 in *Xcr1*$^{Cre–}$ + mFLex and n=13 in *Xcr1*$^{Cre–DTA}$+mFLex group). Biological replicates are shown in all the graphs with the individual data and mean±SEM. **B** and **G**, Two-way repeated measures ANOVA test with Holm-Sidak correction was performed. **C** through **E**, **H**, and **I**, Unpaired *t* test was performed. Exact *P* values are indicated in Supplemental Material III. Gating strategy for flow cytometry analysis is shown in Supplemental Material IV.*$P$<0.05, **$P$<0.01, ****$P$<0.0001.

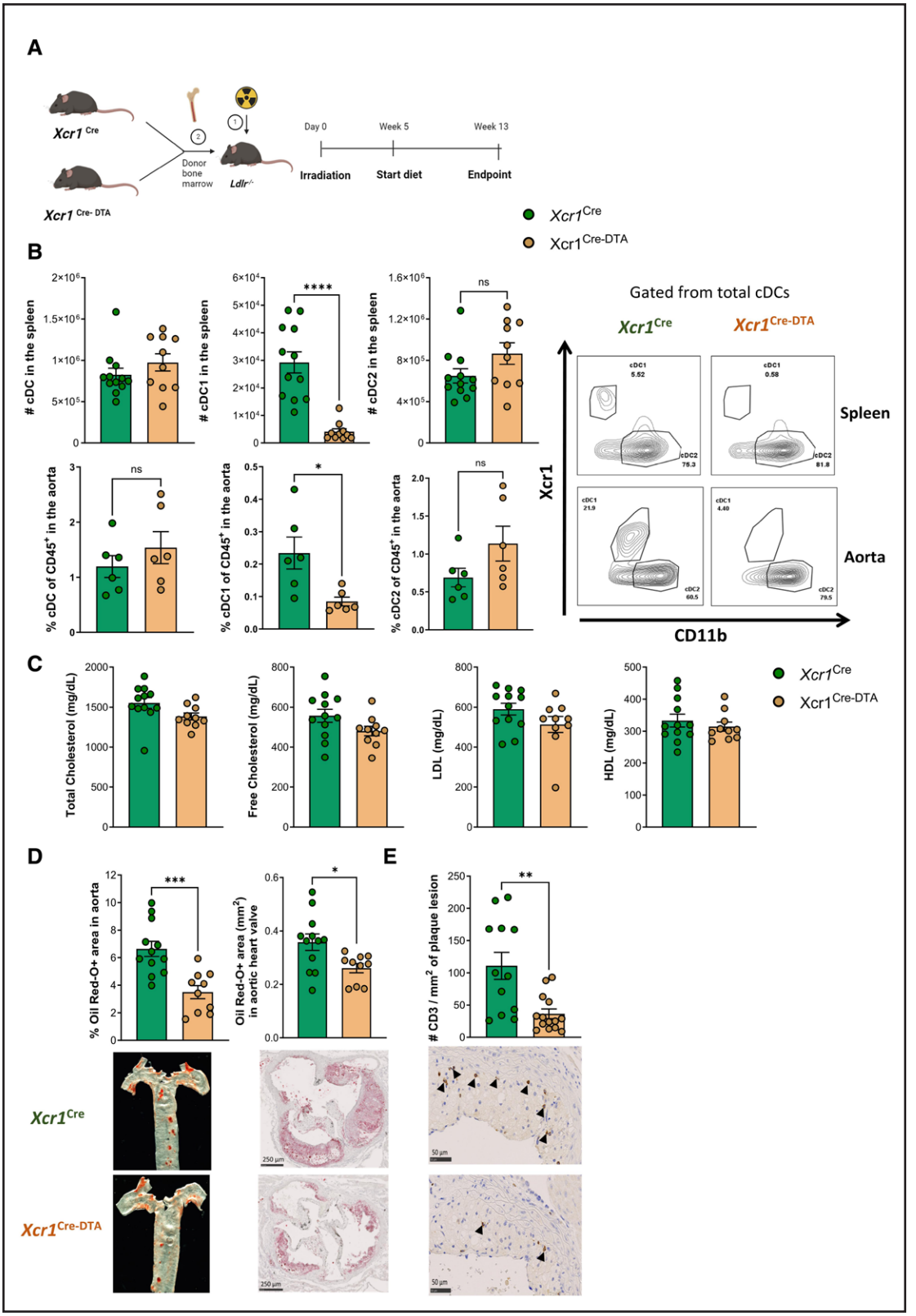


**Figure 2. Conventional type 1 dendritic cell (cDC1) depletion using *Xcr1*$^{Cre–DTA}$ mice reduces atheroma plaque formation.**
**A**, *Ldlr*$^{-/-}$ CD45.1 male mice were grafted with bone marrow (BM) from *Xcr1*$^{Cre}$ or *Xcr1*$^{Cre–DTA}$ donor mice. After BM reconstitution, mice were fed a high-cholesterol diet (HCD) for 8 weeks, followed by euthanasia and analysis. **B**, Flow cytometry analysis of total cDCs (F4/80$^{–}$, CD3$^{–}$, CD19$^{–}$, Ly6c$^{–}$, Ly6G$^{–}$, CD11c$^{+}$, and IA/IE$^{+}$), cDC1s (cDCs, XCR1$^{+}$, and CD11b$^{–}$) and cDC2s (cDCs, XCR1$^{–}$, and CD11b$^{+}$). Spleen numbers (**top left**) and frequencies within CD45$^{+}$ cells in the aorta (**bottom left**) of cDCs, cDC1s, and conventional type 2 dendritic cells (cDC2s) by flow cytometry analyses, showing representative contour plots of the mean (**right**; n=12 in *Xcr1*$^{Cre}$ and n=10 in *Xcr1*$^{Cre–DTA}$ groups for spleen analysis (*Continued*)

profile in the grafted *Ldlr*$^{-/-}$ mice fed HCD (Figure 3C), whereas atherosclerotic lesion in the aorta and the aortic heart valve was significantly reduced (Figure 3D). These results independently confirm that cDC1s contribute to the development of atherosclerosis.

## cDC1s Boost CD4$^+$ Th1 and Cytotoxic CD8$^+$ Immunity at the Atheroma Plaque

Within DCs, cDC1s are superior in priming proinflammatory CD4$^+$ Th1 responses and cytotoxic CD8$^+$ T cells.[35] Given the observed reduction of infiltrating T cells into the aortic heart valve in *Ldlr*$^{-/-}$ chimeric mice with impaired cDC1s (Figure 2D), we further dissected the changes in the infiltrating T-cell population in the aorta of cDC1-impaired compared with control mice by scRNA-seq. To this aim, lethally irradiated *Ldlr*$^{-/-}$ CD45.1 male mice were grafted with *Xcr1*$^{Cre–DTA}$ or control *Xcr1*$^{Cre}$ BM and fed HCD for 8 weeks. At the end point, 10 mice per group were pooled and aortic CD45$^+$ CD3$^+$ CD11c$^-$ IA/IE$^-$ F4/80$^-$ Ly6C$^-$ Ly6G$^-$ NK1.1$^-$ were sorted (Figure S6A) and sequenced. Several 6259 CD3$^+$ T cells were sequenced in *Xcr1*$^{Cre}$ control chimeric mice, while 4072 cells were sequenced in cDC1-impaired *Xcr1*$^{Cre–DTA}$ chimeric mice. Nine different clusters were identified based on the following gene expression profile (Figures 4A and 4B; Figure S6B and S6C): CD4$^+$ Th1 (*Ifng, Tbx21,*), CD4$^+$ Th17 (*Rorc, Il7r, Il17a*), CD4$^+$ Treg (*Foxp3, Il2ra*), naive CD4$^+$ (*Ccr7, Sell*), and stem cell–like memory CD4$^+$ (*Foxp1, Lef1, Foxo1, Klf7*). CD8$^+$ clusters were stratified as cytotoxic CD8$^+$ (*Gzmb, Ifng, Prf11, Tbx21*), naïve CD8$^+$ (*Ccr7, Sell*) and stem cell–like memory CD8$^+$ (*Foxp1, Lef1, Foxo1, Klf7*). One additional cluster of γδT cells (*Trdc, Myb*) was also identified.

CD4$^+$ Th1 cells are associated with a proatherogenic role.[36] In this line, we observed that the chimeric *Ldlr*$^{-/-}$ mice lacking cDC1s had a drastic reduction in the CD4$^+$ Th1 and cytotoxic CD8$^+$ clusters, along with a decrease in CD4$^+$ Tregs possibly as a secondary effect (Figure 4C). CD4$^+$ Th1 polarization is dependent on IL-12.[17] Consistently, IL-12 mRNA expression in aortic CD45$^+$ cells in chimeric *Xcr1*$^{Cre–DTA}$ mice was decreased compared with *Xcr1*$^{Cre}$ BM-grafted *Ldlr*$^{-/-}$ mice (Figure 4D). Notably, IFN (interferon)-γ production was decreased in both CD4$^+$ and CD8$^+$ cells in the spleen (Figure 4E) and restimulation of splenocytes isolated from chimeric mice that lack cDC1 showed impaired IL-12 production (Figure 4F), suggesting that the modulation of immunity by the absence of cDC1s is systemic and not only local in the aorta, as revealed by the scRNA-seq of immune infiltrates in the aorta. CD4$^+$ Treg frequency was also mildly decreased in the spleen, while CD4$^+$ Th17 cells were similar in frequency (Figure S6D).

To assess the degree of clonality of T cells in our scRNA-seq dataset, we analyzed the TCR (T-cell receptor) repertoire using the TRUST4 algorithm, obtaining a total of 1658 cells with TCR information. While this approach provides valuable insights into CD3$^+$ T-cell clonal diversity, the inherent features of 3′ scRNA-seq limit the number of captured TCRs, which could affect the resolution of our clonal analysis. Cells with TCR information were distributed equally in both samples and along all the clusters (Figure S6E). Expectedly, the γδT cell cluster was enriched with TRγ and TRδ sequences, while all other clusters corresponded to αβT cell clusters enriched in TRα and TRβ sequences (Figure S6F). The data analysis showed a lower number of clonotypes and clonal expansion in CD3$^+$ T cells from aorta of *Xcr1*$^{Cre–DTA}$ chimeric mice compared with *Xcr1*$^{Cre}$ BM-grafted *Ldlr*$^{-/-}$ mice (Figure 4G; Figure S6G). Interestingly, some CD4$^+$ Th1 and cytotoxic CD8$^+$ clones were uniquely expanded in control *Xcr1*$^{Cre}$ BM-grafted *Ldlr*$^{-/-}$ mice compared with *Xcr1*$^{Cre–DTA}$ chimeric mice (Figure 4H), suggesting that CD4$^+$ Th1 and cytotoxic CD8$^+$ cell responses were marked by clonal expansion in atherosclerosis and associated with the presence of cDC1s.

## Stimulator of IFN Genes in cDC1s Is Required to Boost Immunity and Contribute to Atherosclerosis

To explore the potential upstream trigger of IL-12 production in cDC1s in the atherosclerosis context, we explored the potential activation of stimulator of IFN genes (STING). STING is a signaling molecule activated downstream of the detection of cytosolic DNA, known to activate IFN regulatory factor 3 and induce type I IFN production and IL-12, among other cytokines.[37] Previous work demonstrated that genetic deletion of STING in *ApoE*$^{-/-}$ reduced atherosclerosis,[38] but the specific role of STING in cDC1s in their induction of atherosclerosis has not been explored.

First, we observed that splenic cDC1s from *Ldlr*$^{-/-}$ mice fed with HCD showed an increase of phosphorylated

**Figure 2 Continued.** and n=6/group in aorta analysis). Each dot in aorta graphs represents a pool of 2 individual aortas. **C**, Total cholesterol, free cholesterol, LDL (low-density lipoprotein), and HDL (high-density lipoprotein) analysis in plasma at end point (n=12 in *Xcr1*$^{Cre}$ and n=10 in *Xcr1*$^{Cre–DTA}$ groups). **D**, Quantification (**top**) and representative images of the mean (**bottom**) of atherosclerotic lesion by Oil Red-O staining of the aorta (**left**) or aortic heart valve (**right**; n=12 in *Xcr1*$^{Cre}$ and n=10 in *Xcr1*$^{Cre–DTA}$ groups). **E**, Staining of CD3$^+$ T cells infiltrating the aortic heart valve lesion showing quantification (**top**) and representative images of the mean (**bottom**; n=12 in *Xcr1*$^{Cre}$ and n=14 in *Xcr1*$^{Cre–DTA}$ groups). Biological replicates are shown in all the graphs with the individual data and mean±SEM. Unpaired *t* test was performed when normal distribution was followed, whereas Mann-Whitney *U* test was applied when non-normal distribution was shown (Supplemental Material III). Exact *P* values are indicated in Supplemental Material III. Gating strategy for flow cytometry analysis is shown in Supplemental Material IV. ns indicates nonsignificant. **P*<0.05; ***P*<0.01; ****P*<0.001; *****P*<0.0001.

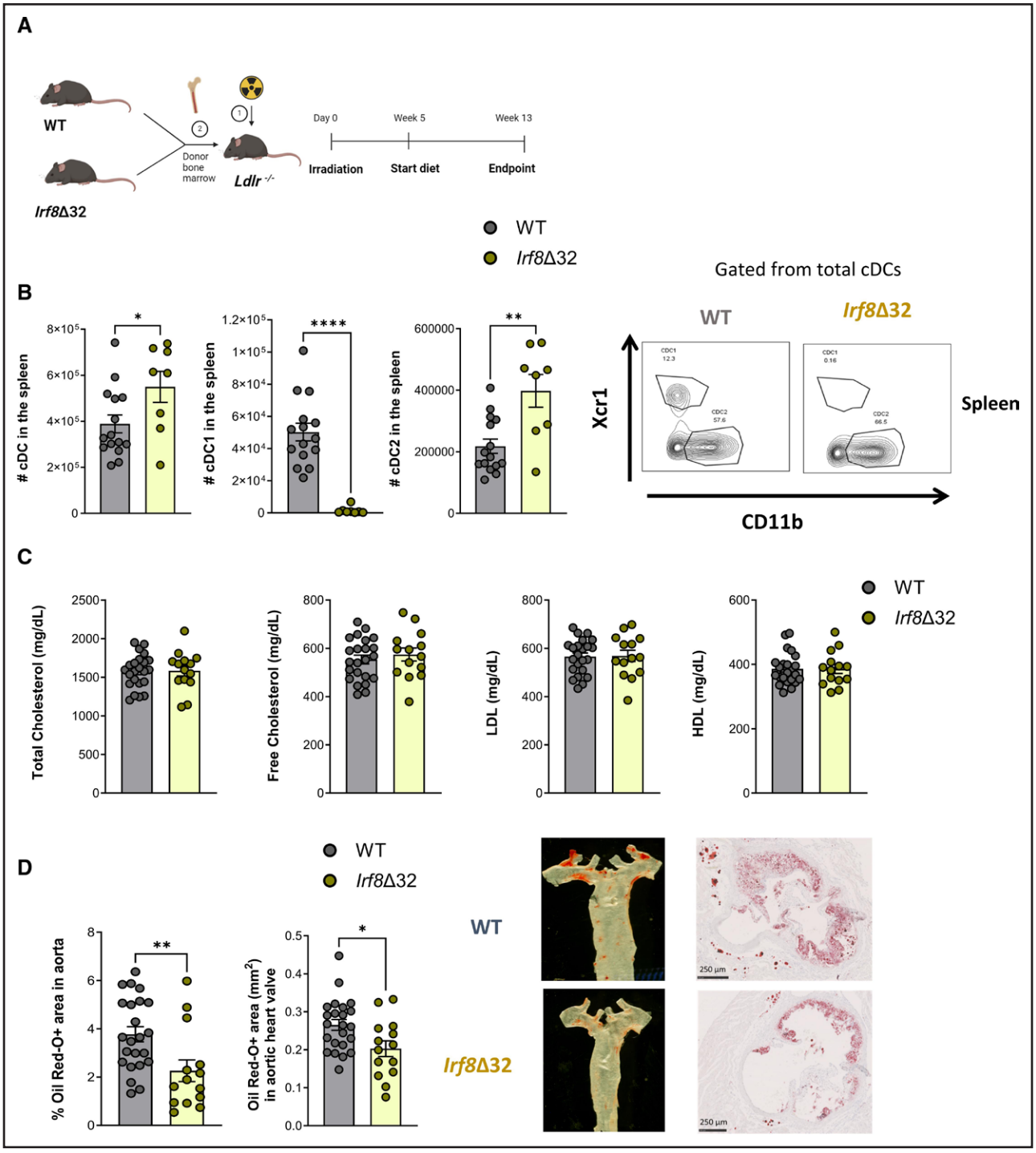


**Figure 3. Conventional type 1 dendritic cells (cDC1) depletion using *Irf8*Δ32 mice reduces atheroma plaque formation.**
**A**, *Ldlr*$^{-/-}$ CD45.1 male mice were grafted with bone marrow (BM) from wild-type (WT) or *Irf8*Δ32 mice. After BM reconstitution mice were fed a high-cholesterol diet (HCD) for 8 weeks, followed by euthanasia and analysis. **B**, Flow cytometry analysis of splenic total cDCs (F4/80$^{-}$, CD3$^{-}$, CD19$^{-}$, Ly6c$^{-}$, Ly6G$^{-}$, CD11c$^{+}$, and IA/IE$^{+}$), cDC1s (cDCs, XCR1$^{+}$, and CD11b$^{-}$) and cDC2s (cDCs, XCR1$^{-}$, and CD11b$^{+}$). Numbers (**left**) and representative contour plots of the mean (**right**) are shown (n=15 in WT and n=8 in *Irf8*Δ32 group). **C**, Total cholesterol, free cholesterol, LDL (low-density lipoprotein), and HDL (high-density lipoprotein) analysis in plasma at end point (n=23 in WT and n=14 in *Irf8*Δ32 group). **D**, Quantification (**left**) and representative images of the mean (**right**) of atherosclerotic lesion by Oil red-O staining of the aorta or aortic heart valve (n=23 in WT and n=14 in *Irf8*Δ32 group). Biological replicates are shown in all the graphs with the individual data and mean±SEM. Unpaired *t* test was performed when normal distribution was followed, whereas Mann-Whitney *U* test was applied when non-normal distribution was shown (Supplemental Material III). Exact *P* values are indicated in Supplemental Material III. Gating strategy for flow cytometry analysis is shown in Supplemental Material IV. **P*<0.05; ***P*<0.01 *****P*<0.0001.

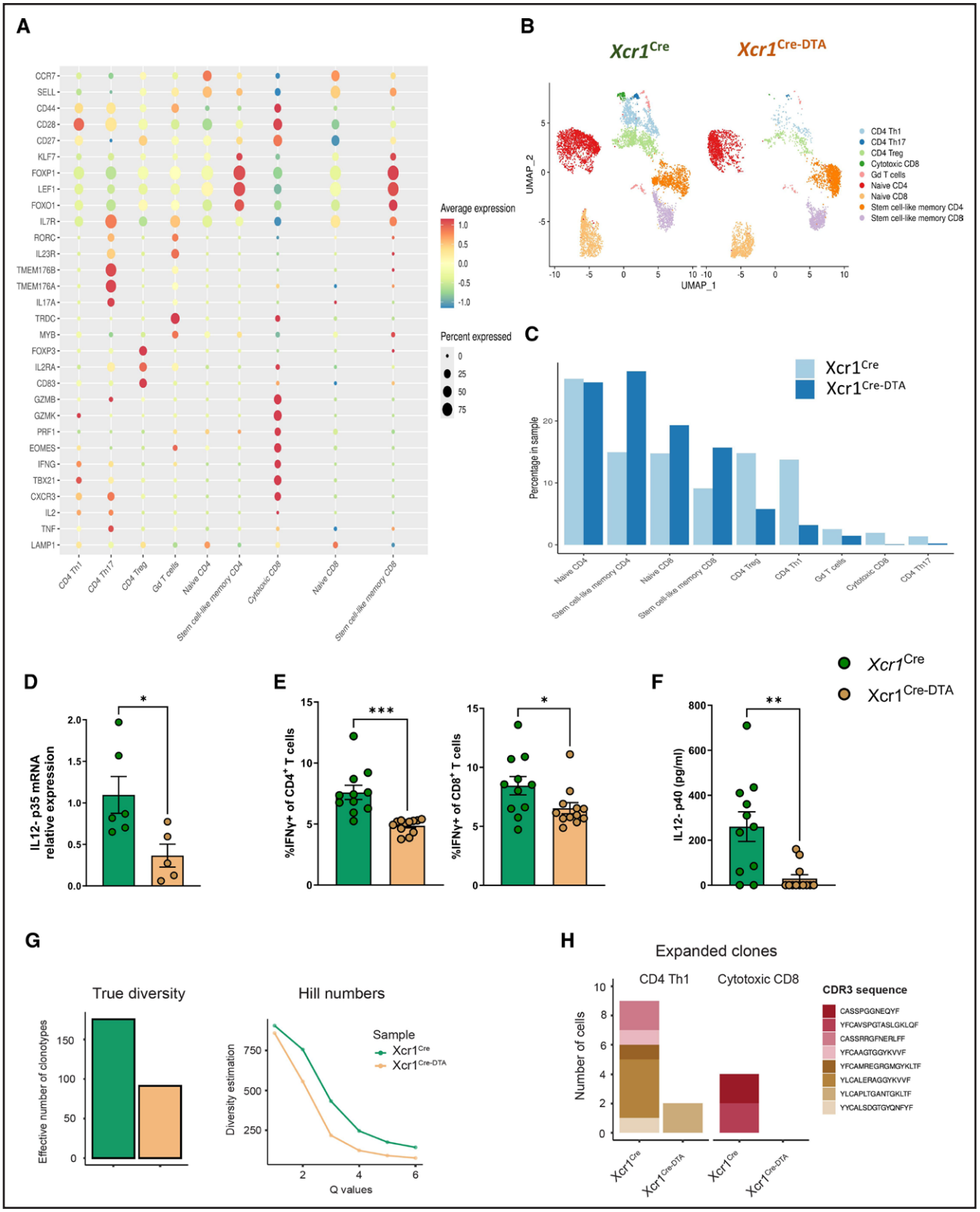


**Figure 4. scRNA-seq analysis of aortic CD3⁺ T cells from atheroma plaque in the presence or absence of conventional type 1 dendritic cells (cDC1s).**

*Ldlr*$^{-/-}$ male mice were grafted with bone marrow from *Xcr1*$^{Cre}$ or *Xcr1*$^{Cre-DTA}$, fed 8 weeks with a high-cholesterol diet (HCD), followed by euthanasia and analysis. **A**, Dot plot of cell type markers used to identify main cell populations in a scRNA-seq analysis on aortic CD3⁺ T cells. **B**, UMAP labeled by cell type of aortic CD3⁺ T cells based on transcriptomic profiles. **C**, Percentage of every cluster identified in both samples. **D**, Analysis of IL (interleukin)-12 mRNA expression by quantitative polymerase chain reaction in aortic CD45+ cells (n=6 in *Xcr1*$^{Cre}$ and n=5 in *Xcr1*$^{Cre-DTA}$ group). Each dot is a pool of 2 aortas. **E**, Flow cytometry analysis of IFN (interferon)-γ production by CD4⁺ (**left**) and (*Continued*)

STING in comparison with splenic cDC1s from *Ldlr*$^{-/-}$ fed with chow diet (Figure S7A). This suggests that, during atherosclerosis disease, there is a systemic STING activation in cDC1s that could contribute to their pro-atherogenic role. To better dissect the role of STING in cDC1s in the context of atherosclerosis, we generated mixed BM chimeras in *Ldlr*$^{-/-}$ recipient mice using 50% BM from C57BL/6J-Sting1$^{gt}$/J (*Tmem173*$^{gt}$) and 50% BM from control *Xcr1*$^{Cre}$ or cDC1-depleted *Xcr1*$^{Cre–DTA}$ mice. STING$^{gt}$ contains an I199N mutation that affects the stability and expression of the protein, fully preventing STING responses (eg, IFN-I production in response to STING agonists).[39] After BM reconstitution (Figure S7B), *Ldlr*$^{-/-}$ chimeric male mice were fed HCD for 8 weeks until end point analysis (Figure 5A). Notably, the numbers of total DCs, cDC1s, and cDC2s were similar between both groups (Figure 5B), suggesting that half-dose of *Tmem173*$^{gt}$ cDC1s in *Xcr1*$^{Cre–DTA}$ reconstitute the whole niche. *Tmem173*$^{gt}$/*Xcr1*$^{Cre}$ chimeric mice have half BM expressing STING$^{gt}$, while the *Tmem173*$^{gt}$/*Xcr1*$^{Cre–DTA}$ chimeric mice are equal than *Tmem173*$^{gt}$/*Xcr1*$^{Cre}$ except for cDC1s that are all STING$^{Gt}$ (Figure 5C). No differences in body weight gain or cholesterol concentration were observed between both groups (Figures 5D; Figure S7C). Of note, only mice in which all cDC1s were mutant STING$^{Gt}$ showed a reduction in aortic plaques (Figure 5E) not caused by a decreased cDC1 number, because the niche was fully reconstituted in both experimental and control mice. Notably, analysis of the spleen at the end point revealed that CD4$^{+}$ Th1 and cytotoxic CD8$^{+}$ immunity decreased when all cDC1s were mutant STING$^{Gt}$ (Figure 5F). These data suggest that intrinsic activation of STING in cDC1s contributes to atherosclerosis progression by priming CD4$^{+}$ Th1 and cytotoxic CD8$^{+}$ immunity.

## Selective Targeting of cDC1s With Dexamethasone-Loaded Nanoparticles Prevents Atherosclerosis Progression

The results showing that cDC1s prime a proatherogenic response led us to hypothesize that specific dampening of the immunogenic activity of cDC1s could reduce atherosclerosis. Dexamethasone is a well-established pharmacological entity that prevents DC immunogenicity.[40] To specifically target cDC1s, we generated liposome-based nanoparticles functionalized with 7H11 anti-CLEC9A antibody which specifically binds to DNGR-1/CLEC9A, a C-type lectin-like receptor with selective high expression in cDC1s.[12] In addition, to reduce the immunogenic capacity of cDC1s, these cDC1-targeted- nanoparticles were loaded with dexamethasone (Figure 6A).

The mean hydrodynamic diameter and polydispersity index of liposome batches before (LP) and after drug loading (LP$_{DEXA}$) and antibody coupling (LP-CLEC9A and LP$_{DEXA}$-CLEC9A) demonstrated an adequate size for intravenous administration (Figure S8A). Dexamethasone concentrations loaded into nanoparticles were calculated and showed similar loading in LP$_{DEXA}$ and LP$_{DEXA}$-CLEC9A (Figure S8B).

To test cDC1 targeting, *Ldlr*$^{-/-}$ mice were injected intravenously with fluorescent DiR-labeled nanoparticles decorated (LP$_{DEXA}$-CLEC9A) or not (LP$_{DEXA}$) with 7H11 anti-CLEC9A and their uptake by splenic cDC1s, cDC2s, macrophages, and monocytes was analyzed by flow cytometry detection of DiR. LP$_{DEXA}$-CLEC9A targeted around 60% of cDC1s while were hardly detected in cDC2s, macrophages, or monocytes. Control LP$_{DEXA}$ showed some uptake by macrophages but was not found in cDC1s, cDC2s, or monocytes (Figure 6B). To test the effect of LP$_{DEXA}$-CLEC9A in cDC1s, we stimulated in vivo with PolyI:C, an agonist of endosomal TLR3 (toll-like receptor 3) highly expressed in cDC1s. LP$_{DEXA}$-CLEC9A decreased the expression of costimulatory molecules CD80 and CD40 in response to PolyI:C in comparison with LP-CLEC9A, suggesting reduced cDC1 immunogenicity (Figure S8C).

To test whether LP$_{DEXA}$-CLEC9A could be used to specifically attenuate the immunogenicity of cDC1s in the context of atherosclerosis, *Ldlr*$^{-/-}$ male mice were fed with HCD for 8 weeks and administered intravenous LP, LP-CLEC9A, LP$_{DEXA}$-CLEC9A, or LP$_{DEXA}$ twice weekly in the last 4 weeks (Figure 6C). None of these nanoparticles is influenced by body weight (Figure 6D). Remarkably, mice treated with LP$_{DEXA}$-CLEC9A showed less atherosclerosis in the aorta and the heart valve (Figure 6E) compared with all other groups. Because LP$_{DEXA}$ administration did not affect atherosclerosis progression, these data suggest that specific delivery of dexamethasone to cDC1s is required to reduce atherosclerosis. Of note, the reduction in atherosclerosis lesions observed on LP$_{DEXA}$-CLEC9A administration was independent of the lipid profile (Figure 6F), and we did not find an increase in plasma biomarkers related to hepatic (ALT/GPT, AST/GOT, total bilirubin) or renal damage (ureic nitrogen, phosphorus) in mice treated with any of these nanoparticles (Figure S8D).

Systemic administration of nanoparticles intravenously also resulted in changes in splenic CD4$^{+}$ and CD8$^{+}$ T cells. Mice treated with LP$_{DEXA}$-CLEC9A showed

**Figure 4 Continued.** CD8$^{+}$ (**right**) T cells in phorbol 12-myristate 13-acetate (PMA)–restimulated splenocytes (n=12 in *Xcr1*$^{Cre}$ and n=11 in *Xcr1*$^{Cre–DTA}$ group). **F**, IL-12 concentration measured by ELISA in the supernatant of PMA-restimulated splenocytes (n=12 in *Xcr1*$^{Cre}$ and n=11 in *Xcr1*$^{Cre–DTA}$ group). **G**, TCR (T-cell receptor) analysis of aortic CD3$^{+}$ T cells. Effective number of clonotypes (**left**) and diversity estimation by Hill numbers (**right**). **H**, Analysis of expanded clones and its CDR3 sequence in CD4$^{+}$ Th1 and cytotoxic CD8$^{+}$ clusters. Biological replicates are shown in all the graphs with the individual data and mean±SEM. **D** through **F**, Mann-Whitney *U* test was performed. Exact *P* values are indicated in Supplemental Material III. Gating strategy for flow cytometry analysis is shown in Supplemental Material IV. **P*<0.05; ***P*<0.01; ****P*<0.001.

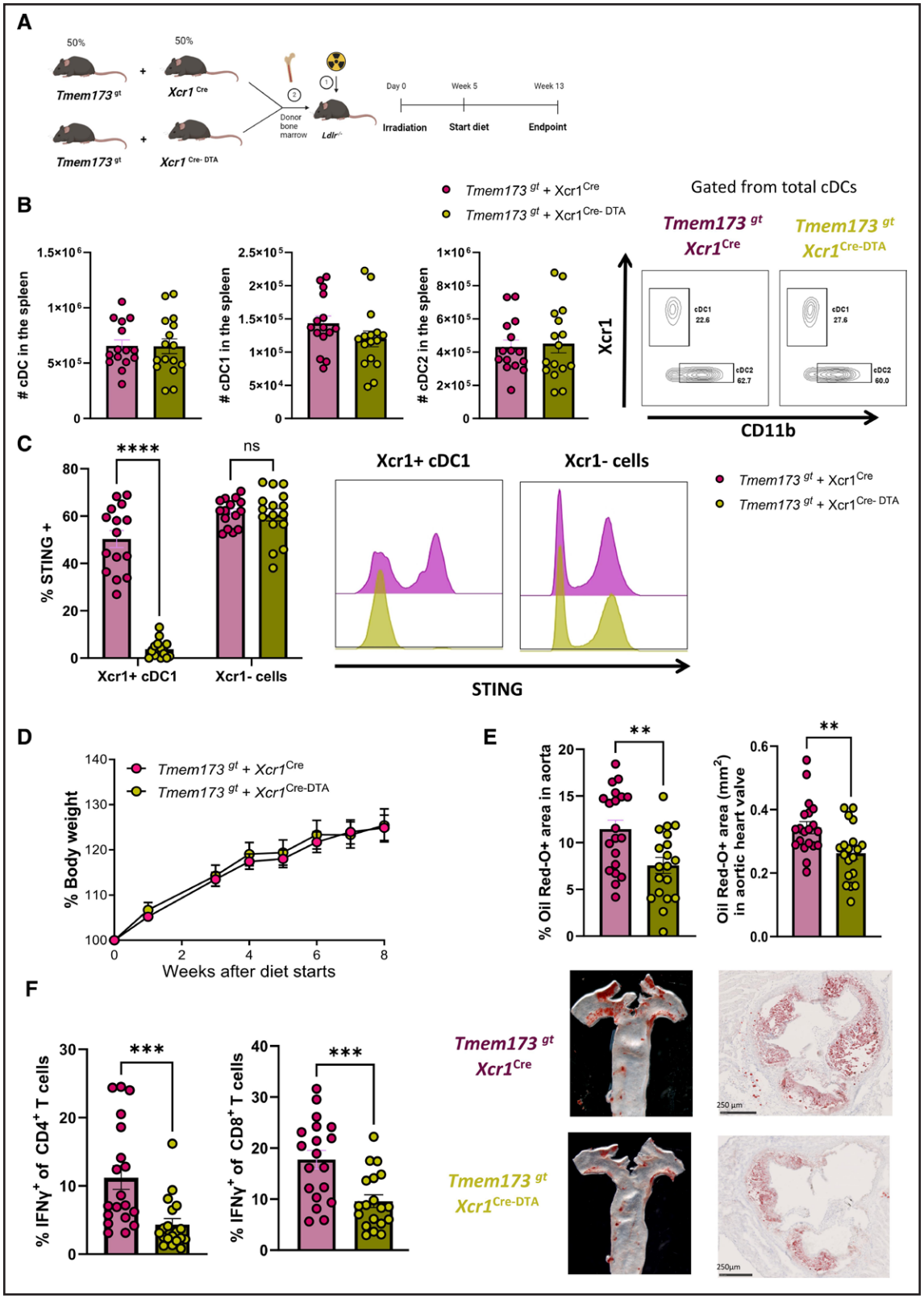


**Figure 5. Stimulator of IFN (interferon) genes (STING) in conventional type 1 dendritic cells (cDC1s) is required to boost immunity and contributes to atherosclerosis.**

**A**, *Ldlr*$^{-/-}$ CD45.1 male mice were grafted with 50% of bone marrow (BM) from *Tmem173*$^{gt}$ and 50% from *Xcr1*$^{Cre}$ or *Xcr1*$^{Cre–DTA}$ mice. After BM reconstitution mice were fed with high-cholesterol diet (HCD) for 8 weeks, followed by euthanasia and analysis. **B**, Flow cytometry analysis of total cDCs (F4/80$^{-}$, CD3$^{-}$, CD19$^{-}$, Ly6c$^{-}$, Ly6G$^{-}$, CD11c$^{+}$, IA/IE$^{+}$), cDC1s (cDCs, XCR1$^{+}$, CD11b$^{-}$) and conventional type 2 dendritic cells (cDC2s; cDCs, XCR1$^{-}$, CD11b$^{+}$) in spleen. Numbers (**left**) and representative contour plots of the mean (*Continued*)

a reduction in CD4+ Th1 cells compared with all other groups (Figure 6G). CD8+ IFN-γ + cells decreased with $LP_{DEXA}$-CLEC9A compared with LP and LP-CLEC9A but showed no significant difference compared with $LP_{DEXA}$. No changes were observed in CD4+ Tregs or CD4+ Th17 cells (Figure 6G).

Finally, given the immunosuppressive capacity of $LP_{DEXA}$-CLEC9A nanoparticles, we tested whether administration of these nanoparticles could affect antiviral immunity. For this purpose, LP-CLEC9A or $LP_{DEXA}$-CLEC9A nanoparticles were injected in *Ldlr*$^{-/-}$ mice 7 and 4 days before intranasal infection with PR8 influenza virus, and body weight was monitored along the experiment. In addition, blood was collected 8 days after viral infection to analyze antigen-specific immune response against PR8 virus (Figure S8E). We observed that mice treated with LP-CLEC9A or $LP_{DEXA}$-CLEC9A showed no differential morbidity to viral infection by weight change (Figure S8F). Antiviral effector immunity was similar, with similar total, naive (CD44− CD62L+), central memory (CD44+ CD62L+), and effector (CD44+ CD62L−) CD8+ T cells in blood 8 days postviral infection. Moreover, specific antigen response against PR8 influenza virus epitope in effector CD8+ T cells was equal, measured by H2-Db-PR8 influenza A nucleoprotein tetramer (Figure S8G).

These results demonstrate that specific targeting to cDC1s with $LP_{DEXA}$-CLEC9A impairs cDC1 priming of immunity, reducing atherosclerosis plaque formation in the absence of potential side effects, such as liver and renal damage or a reduction to antiviral immunity.

## DISCUSSION

Although the involvement of adaptive immunity in atherosclerosis is well established,[2–4] the precise role of DCs and, particularly, different subsets within DCs is controversial.[22–24,26–28] The role of DCs in atherosclerosis has been previously addressed using either *Flt3*$^{-/-}$, *Batf3*$^{-/-}$ or *Itgax-Cre Irf8*$^{f/f}$ models to deplete cDC1s in atheroprone *Ldlr*$^{-/-}$ or *ApoE*$^{-/-}$ mice. However, although in all these models, CD8α+ cDC1s and aortic CD11b− CD103+ cDC1s were depleted, the results in atherosclerosis progression were contradictory, showing that cDC1 depletion resulted in an increase,[22] decrease,[23,24,26] or no effect[27,28] of atherosclerosis lesion. Herein, we have used alternative approaches combining strategies for gain and loss of function of cDCs and particularly cDC1s to address their role in atherosclerosis. As a gain-of-function approach, we expanded all DC subsets by hydrodynamic injection of the mFLex plasmid expressing FLT3L[33] and found an increase in atherosclerosis, indicating that at least 1 DC subset promotes atherosclerosis and cannot be compensated by a protective role of any other expanded DC subset. We then asked the question of which DC subtype could be responsible for this phenotype. Although BATF3-deficiency has been used extensively in the literature to deplete cDC1s, this model has several caveats.[41–43] We thus used 2 different models to deplete specifically cDC1s: a flox STOP-DTA under the control of *Xcr1*-Cre driver and the *Irf8*Δ32 mice that specifically target IRF8-dependent cDC1 development. Of note, the increased atherosclerosis on mFLex expansion was prevented by cDC1 depletion. Moreover, even in the absence of mFLex and DC expansion, cDC1 depletion using the *Xcr1*$^{Cre–DTA}$ model decreased HCD-induced atherosclerosis in grafted *Ldlr*$^{-/-}$ male and female mice. This atheroprone effect of cDC1s was validated in *Ldlr*$^{-/-}$ mice grafted with *Irf8*Δ32 or control BM and fed HCD. These results support a proatherogenic role for cDC1s.[23,24,26] Mechanistically, our combined gain and loss of function approaches suggest that cDC1s prime a proatherogenic CD4+ Th1 and cytotoxic CD8+ T-cell immunity. IL-12 is a key CD4+ Th1 cell polarizing[17] and CD8+T-cell activating cytokine produced by cDC1s.[16] In our work, the decrease in CD4+ Th1 and CD8+T-cell response correlated with lower IL-12 production in the aortas and spleens of cDC1-deficient mice. Regarding cDC1 activation in atherosclerosis to provide IL-12 proatherogenic cytokine, we found that STING in cDC1s is needed for their proatherogenic function. STING regulates the activation of cDC1s through the detection of cytosolic DNA and subsequent production of type I IFNs and other cytokines, including IL-12.[44] In other cardiovascular diseases, such as obesity, cDC1s from white adipose tissue uptake self-DNA from apoptotic bodies and produce IL-12 in a STING dependent manner. Consistent with our findings in atherosclerosis, cDC1 depletion through diphtheria toxin injection in *Xcr1*$^{DTR}$ mice fed a high-fat diet reduced obesity-related inflammation by limiting IL-12 production.[37]





**Figure 5 Continued.** (**right**; n=15 in *Tmem173*$^{gt}$ *Xcr1*$^{Cre}$ and 16 in *Tmem173*$^{gt}$ *Xcr1*$^{Cre–DTA}$ group). **C**, Flow cytometry analysis of STING in cDC1s and XCR1− cells showing quantification (**left**) and representative histogram of the mean (**right**; n=15 in *Tmem173*$^{gt}$ *Xcr1*$^{Cre}$ and 16 in *Tmem173*$^{gt}$ *Xcr1*$^{Cre–DTA}$ group). **D**, Percentage of body weight tracked for 8 weeks of HCD (n=20 in *Tmem173*$^{gt}$ *Xcr1*$^{Cre}$ and 19 in *Tmem173*$^{gt}$ *Xcr1*$^{Cre–DTA}$ group). **E**, Quantification (**top**) and representative images of the mean (**bottom**) of atherosclerotic lesion by Oil Red-O staining of the aorta (**left**) or aortic heart valve (**right**; n=20 in *Tmem173*$^{gt}$ *Xcr1*$^{Cre}$ and 19 in *Tmem173*$^{gt}$ *Xcr1*$^{Cre–DTA}$ group). **F**, Flow cytometry analysis of IFN-γ production by CD4+ (**left**) and CD8+ (**right**) T cells in phorbol 12-myristate 13-acetate–restimulated splenocytes (n=19 in both groups). Biological replicates are shown in all the graphs with the individual data and mean±SEM. **D**, 2-way repeated measures ANOVA test with Holm-Sidak correction was performed. For the other panels, Unpaired *t* test was performed when normal distribution was followed, whereas Mann-Whitney *U* test was applied when non-normal distribution was shown (Supplemental Material III). Exact *P* values are indicated in Supplemental Material III. Gating strategy for flow cytometry analysis is shown in Supplemental Material IV. ns indicates nonsignificant. ***P*<0.01; ****P*<0.001 *****P*<0.0001.

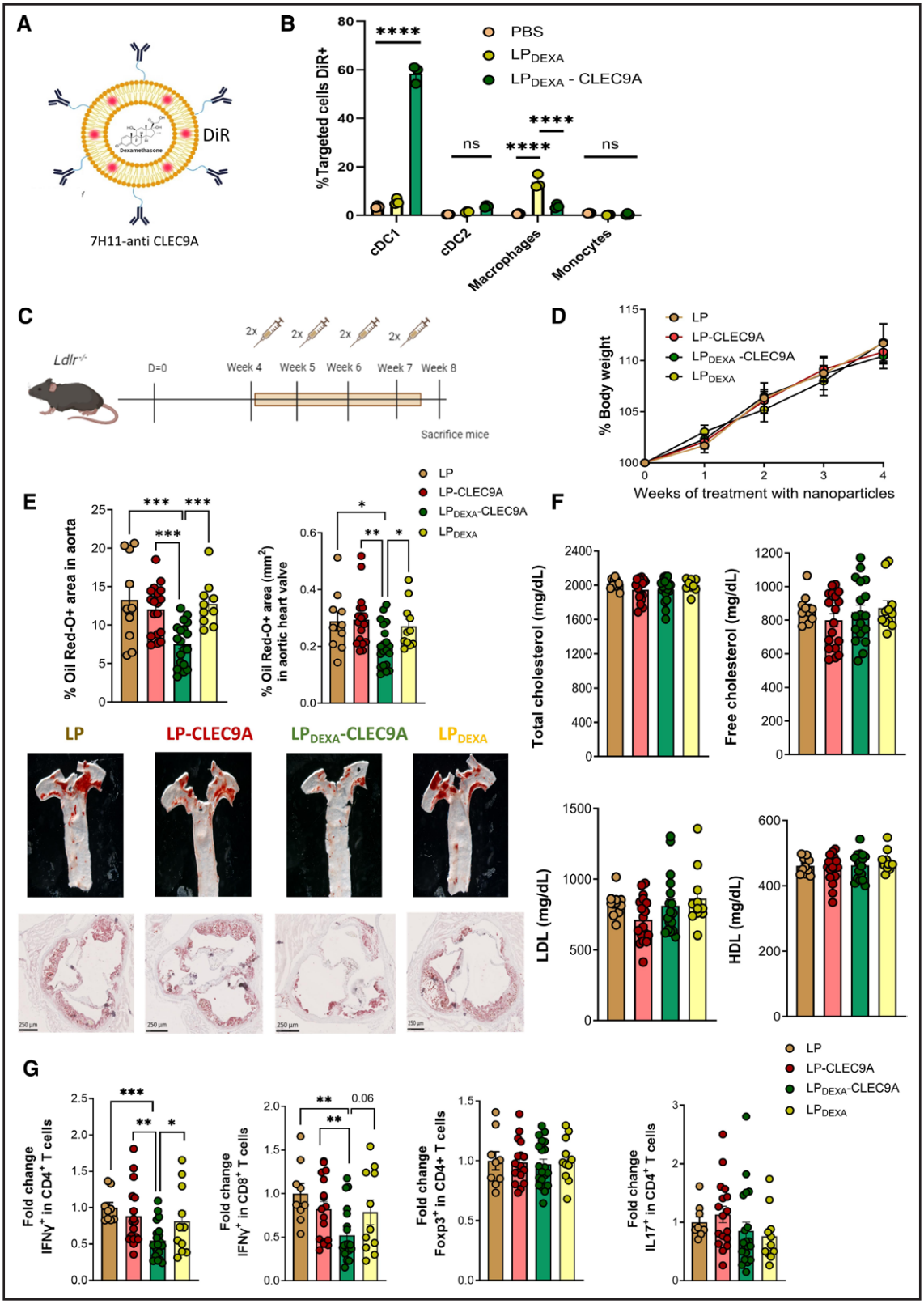


**Figure 6. Selective targeting of conventional type 1 dendritic cells (cDC1s) with dexamethasone-loaded nanoparticles prevents atherosclerosis progression.**

**A**, Scheme of the synthesized nanoparticles (NPs) loaded with dexamethasone (DEXA) in the aqueous cavity, labeled with fluorescent DiR dye and covalently coupled to 7H11 anti-CLEC9A antibody to specifically target cDC1. **B**, Flow cytometry analysis of cell-specific targeting by $LP_{DEXA}$ or $LP_{DEXA}$-CLEC9A to cDC1s ($CD11c^+$, $IA/IE^+$, $XCR1^+$, and $CD11b^-$), cDC2s ($CD11c^+$, $IA/IE^+$, $XCR1^-$, and $CD11b^+$), macrophages ($CD64^+$ and $F4/80^+$), or monocytes ($F4/80^-$, $CD3^-$, $CD19^-$, and $Ly6c^+$) in spleen 24 hours after intravenous injection of NPs. Targeted cells (*Continued*)

Although our results using these gain and loss of function approaches suggest that cDC1s are proatherogenic, there are potential explanations for the differences between our results and previous studies suggesting different roles for cDC1s in the context of atherosclerosis. On the one hand, FLT3L is a key cytokine for the development of all cDCs (cDC1 and cDC2) and also plasmacytoid DCs.[6] The absence of FLT3L sensing in *Flt3*$^{-/-}$ mice would affect the development of all these subsets and favoring the occupation of the niche by other monocyte-derived DCs that may be proinflammatory, making it difficult to associate the phenotype observed only to the absence of cDC1s. In fact, the number of CD4$^+$ Tregs in *Flt3l*$^{-/-}$ mice is already reduced[45] in steady-state conditions suggesting that FLT3/FLT3L axis is needed for an appropriate CD4$^+$ Treg generation. Because CD4$^+$ Tregs are associated with atheroprotection,[46,47] the reduction in CD4$^+$ Tregs caused by the disbalance in DC composition in *Flt3*$^{-/-}$ model could explain the increase in atherosclerosis under cDC1 depletion in the previous work.[22] On the other hand, the use of *Batf3*$^{-/-}$ mice to model cDC1 depletion has been useful in the past, but results in the past years have shown some limitations. First, BATF3 deficiency can be compensated by other transcription factors during cDC1 development under inflammatory conditions, being the deficiency in this subset is partial.[48,49] Moreover, BATF3 has intrinsic functions in T cells. For instance, BATF3 regulates CD8$^+$ T-cell memory development.[41,42] This limitation was observed in previous reports in the context of atherosclerosis, where percentages of memory effector CD8$^+$ T cells were reduced in *Ldlr*$^{-/-}$ *Batf3*$^{-/-}$ compared with *Ldlr*$^{-/-}$ mice.[27] In addition, BATF3 also has an intrinsic role in CD4$^+$ T cells by repressing Foxp3 expression and inhibiting CD4$^+$ Treg differentiation,[41] with *Batf3*$^{-/-}$ mice displaying increased CD4$^+$ Tregs in homeostasis. In this way, the protective role of cDC1 deficiency in *Batf3*$^{-/-}$ mice could be attenuated by all these limitations, explaining previous works that state that cDC1s do not contribute to atherosclerosis disease.[27,28] All these limitations could also justify the contradictory results with others reports that suggest a proatherogenic role of cDC1s based on the use of Batf3-deficient mice[26] or similar models to deplete cDC1s such as *Itgax-Cre Irf8*$^{f/f}$.[23] However, although *Itgax-Cre Irf8*$^{f/f}$ model reduces cDC1 numbers, CD11c is not only expressed on DCs but also foamy macrophages in the aorta,[50] which use IRF8 to regulate IFN-γ production, a key contributing factor in atherosclerosis.[51] Consequently, the specific role of cDC1s cannot be evaluated with *Itgax-Cre Irf8*$^{f/f}$ model. Interestingly, like our results, they also observed a reduction of atheroprotective splenic CD4$^+$ Tregs in *Itgax-Cre Irf8*$^{f/f}$ compared with control. We hypothesize that the suppression of proatherogenic CD4$^+$ Th1 and cytotoxic CD8$^+$ T responses outweighs the loss of atheroprotective CD4$^+$ Tregs, resulting in a reduction of atherosclerosis after cDC1 depletion. In that line, the increase of atheroprotective IL-10 secretion by CD4$^+$ Treg without affecting proatherogenic IFN-γ production in *Ldlr*$^{-/-}$ grafted with *Clec9a*$^{-/-}$ BM reduced atherosclerosis disease.[24] Given the limitations of previous models to target cDC1s, the new approaches described in this work that combine DCs expansion with new models to deplete cDC1s not described before in the context of atherosclerosis, help to better define their function in atherosclerosis.

Lipid-lowering therapy is used to treat atherosclerosis, with statins (inhibitors of cholesterol synthesis) as the therapy of choice both in primary and secondary prevention for cardiovascular diseases. However, the rate of cardiovascular events remains high despite good cholesterol control. Moreover, high doses of statins used to treat cardiovascular diseases can cause secondary effects, including type 2 diabetes onset, neurological and neurocognitive effects, hepatotoxicity, and renal toxicity, among others, resulting in reduced adherence to the treatment and even in intolerance for up to 20% of patients.[52] Alternative pharmacological agents target lipid metabolism (ie, fibrates, cholesterol absorption inhibitors, bile acid sequestrants, PCSK9 [proprotein convertase subtilisin/kexin type 9] inhibitors) and, more recently, inflammation (ie, canakinumab in clinical trials) are emerging.[1,53] However, the adverse effects or their cost per patient have limited their use to specific cases, generally in combination

**Figure 6 Continued.** were analyzed as % DiR$^+$ in each population (N=3/group). Gate for DiR$^+$ cells was defined based on FMO staining. **C**, Scheme of NP-based immunotherapy for atherosclerosis. *Ldlr*$^{-/-}$ male mice were fed with a high-cholesterol diet (HCD) for 8 weeks. During the last 4 weeks of diet, mice were treated twice weekly with LP, LP-CLEC9A, $LP_{DEXA}$-CLEC9A, or $LP_{DEXA}$ by intravenous injection, followed by euthanasia and analysis. **D**, Percentage of body weight tracked during the NP treatment (last 4 weeks of HCD) relative to the initial weight at week 4 (n=10 in LP, n=20 in LP-CLEC9A, n=20 in $LP_{DEXA}$-CLEC9A and n=11 in $LP_{DEXA}$ groups). **E**, Quantification (**top**) and representative images of the mean (**bottom**) of atherosclerotic lesion by Oil Red-O staining of the aorta (**left**) or aortic heart valve (**right**; n=10 in LP, n=18 in LP-CLEC9A, n=20 in $LP_{DEXA}$-CLEC9A and n=11 in $LP_{DEXA}$ groups). **F**, Total cholesterol, free cholesterol, LDL (low-density lipoprotein), and HDL (high-density lipoprotein) analysis in plasma at end point (n=10 in LP, n=18 in LP-CLEC9A, n=18 in $LP_{DEXA}$-CLEC9A and n=11 in $LP_{DEXA}$ groups). **G**, Flow cytometry analysis of IFN (interferon)-γ production by CD4$^+$ (far **left**), CD8$^+$ (**middle left**), Foxp3$^+$ (**middle right**), and IL (interleukin)-17$^+$ (**right**) CD4$^+$ T cells in phorbol 12-myristate 13-acetate/ionomycin-restimulated splenocytes (n=10–20/group). Fold change induction to normalize among independent experiments was calculated using the LP group as control (n=9 in LP, n=17 in LP-CLEC9A, n=20 in $LP_{DEXA}$-CLEC9A and n=11 in $LP_{DEXA}$ groups). Biological replicates are shown in all the graphs with the individual data and mean±SEM. **B**, Two-way ANOVA with Holm-Sidak correction for multiple comparison was performed. **D**, Two-way repeated measures ANOVA test with Holm-Sidak correction was performed. For the other part labels, ordinary 1-way ANOVA with Holm-Sidak correction was performed when normal distribution was followed, whereas Kruskal-Wallis test with Benjamini, Krieger, and Yekutieli correction was applied when non-normal distribution was shown (Supplemental Material III). Exact *P* values are indicated in Supplemental Material III. Gating strategy for flow cytometry analysis is shown in Supplemental Material IV. ns indicates nonsignificant. **P*<0.05; ***P*<0.01; ****P*<0.001 *****P*<0.0001.

with statins. In conclusion, we urgently need alternative approaches to tackle atherosclerosis in a more comprehensive and accessible way, possibly synergizing with current lipid-lowering approaches. Thus, new strategies targeting the immune component of atherosclerosis can be a useful addition to the therapeutic options for this disease and could probably be combined with lipid-lowering therapies. Given the proatherogenic role of cDC1s observed in this study, targeting these cells to reduce their immunogenicity and enhance their tolerogenic properties presents a promising immunotherapy for atherosclerosis. Here, we have shown that nanoparticles containing an immunosuppressive drug like dexamethasone and specifically directed to cDC1s reduced atherosclerotic lesions by decreasing $CD4^+$ Th1 and cytotoxic $CD8^+$ T-cell responses without inducing systemic toxicity. Our study supports the concept that reprogramming cDC1s by reducing its immunogenic phenotype can attenuate the inflammatory environment of atherosclerotic lesions and that this could be used as a novel immunotherapy for atherosclerosis. As a limitation, this immunotherapy not only targets proatherogenic cDC1s, but all cDC1s, which could result in systemic immunosuppression, although we have not found a relevant effect in resistance to influenza infection. For that reason, further studies are needed to direct locally these nanoparticles to the atheroma plaque to avoid side effects. In addition, because this therapy targets the immune component of atherosclerosis, it could be potentially combined with existing lipid-lowering therapies for an additive or synergic effect.

In conclusion, our data demonstrate a proatherogenic role of cDC1s by controlling IFN-γ production in $CD4^+$ Th1 and cytotoxic $CD8^+$ T cells, dependent on the activation of the STING pathway in cDC1s. Our data suggest an important role of cDC1s in promoting the pathogenesis of atherosclerosis and offer a new target for immunotherapy for atherosclerosis.

## ARTICLE INFORMATION

Received October 30, 2024; revision received May 9, 2025; accepted May 19, 2025.

### Affiliations

Centro Nacional de Investigaciones Cardiovasculares Carlos III (CNIC), Madrid, Spain (M.G., V.N., M.F.-M., P.F.-B., E.M.-R., S.M.-C., E.H.-G., M.R.-T., A.R.-R., C.R.-R., A.B., A.D., A.R.R., I.R.-V., D.S.). Escuela de Doctorado, Universidad Autónoma de Madrid, Spain (M.G., E.M.-R., A.R.-R., C.R.-R.). CIC biomaGUNE, Basque Research and Technology Alliance (BRTA), San Sebastian, Spain (L.F.-M., S.C.-R., J.R.-C.). Euskal Herriko Unibertsitatea (UPV/EHU), Donostia, Spain (L.F.-M., S.C.-R., J.R.-C.). Escuela de Doctorado (M.F.-M.) and Departamento de Química en Ciencias Farmacéuticas (J.R.-C.), Universidad Complutense de Madrid, Spain. Inmunotek S.L., Alcalá de Henares, Spain (S.M.-C.). Innate Immune Biology Laboratory, Institute for Research in Biomedicine (IRB Barcelona), The Barcelona Institute of Science and Technology (BIST), Spain (S.K.W.). Aix Marseille Université, INSERM, CNRS, Centre d'Immunologie de Marseille-Luminy, France (S.H., B.M.). INSERM, Centre d'Etude des Pathologies Respiratoires (CEPR), UMR 1100, Université de Tours, France (S.H.). Department of Pathology and Immunology, Washington University School of Medicine, St. Louis, MO (S.J., T.-T.L., K.M.M.). Ikerbasque, Basque Foundation for Science, Bilbao, Spain (S.C.-R., J.R.-C.). CIBER de Enfermedades Respiratorias (CIBERES), Madrid, Spain (S.C.-R., J.R.-C.).

### Acknowledgments

The authors thank the members of the D. Sancho laboratory for their help with discussions and critical reading of the manuscript. In particular, the authors thank Gillian Dunphy for helping the with editing English of the manuscript. The authors thank the Centro Nacional de Investigaciones Cardiovasculares Carlos III facilities, foremost the animal, cellomics, histology, genomics, microscopy, and personnel for their assistance. M. Galán, I. Robles-Vera, and D. Sancho conceptualized and designed the study. M. Galán, L. Fernández-Méndez, M. Femenía-Muiña, E. Moya-Ruiz, S. Martínez-Cano, E. Hernández-García, A. Rodríguez-Ronchel, I. Robles-Vera, V. Núñez, P. Figuera-Belmonte, M. Rodrigo-Tapias, C. Relaño-Rupérez, S.K. Wculek, and A. Benguria performed the experiments and analyzed the data. A. Dopazo, S. Henri, B. Malissen, K.M. Murphy, A.R. Ramiro, S. Carregal-Romero, J. Ruiz-Cabello, S. Jo, T-T. Liu supported the experiments and provided equipment and reagents. D. Sancho, J. Ruiz-Cabello, and A.R. Ramiro acquired funding. D. Sancho and I. Robles-Vera supervised the project. M. Galán and D. Sancho wrote the manuscript with input from all of the authors. All of the authors edited the manuscript and approved the final manuscript.

### Sources of Funding

M. Galán is funded by Becas de Formación del Profesorado Universitario fellowship (FPU) (FPU20/01418). E. Moya-Ruiz and A.R. Ramiro are fellows of the research training program funded by Ministerio de Ciencia, Innovación y Universidades (MICIU; PRE2022-103324 and PRE2020-091873 respectively) I. Robles-Vera is funded by FJC2021-048099-I funded by MCIU/AEI/10.13039/501100011033 and European Union NextGenerationEU/PRTR. M. Femenía-Muiña received the support of a fellowship from the la Caixa Foundation (ID 100010434) under the code LCF/BQ/DR24/12080010. Work in the D. Sancho laboratory is funded by the Centro Nacional de Investigaciones Cardiovasculares Carlos III (CNIC); MICIU PID2022-137712OB-I00, CPP2021-008310 and CPP2022-009762 MICIU/AEI/10.13039/501100011033 Agencia Estatal de Investigación, Unión Europea NextGenerationEU/PRTR; Comunidad de Madrid (P2022/BMD-7333 INMUNOVAR-CM); Scientific Foundation of the Spanish Association Against Cancer (AECC-PRYGN246642SANC); Worldwide Cancer Research (WWCR-25-0080); European Union ERC-2023-PoC; a research agreement with Inmunotek S.L.; and la Caixa Foundation (LCF/PR/HR23/52430012 and LCF/PR/HR22/52420019). Work in the J. Ruiz-Cabello laboratory is funded by MCIN/AEI/10.13039/501100011033 (PID2021-123238OB-I00). J. Ruiz-Cabello received funding from the La Caixa Foundation (Health Research Call 2020: LCF/PR/HR20/52400015), Basque Government under the Elkartek 2024 Program (bmG24), and R&D Projects in Health (grant no. 2022333041) Work in the S. Carregal-Romero laboratory is funded by MCIU/AEI 10.13039/501100011033 projects (CNS2023-143944, RYC2020-030241-I, PID2022-142842OB-I00), the Ikerbasque (Basque Foundation for Science) and Ramon Areces Foundation (CIVP21S13151). Work in the A.R. Ramiro Lab is funded by CNIC, MCIN/AEI 10.13039/501100011033 PID2022-139218OB-I00 project, La Caixa Foundation (LCF/PR/HR22/52420019), Comunidad Autónoma de Madrid (P2022/BMD-7333 INMUNOVAR-CM) and Horizon Europe ERA4HEALTH Cardinnov (MARGINALIZE-MI AC23_2/00007). The CNIC is supported by the Instituto de Salud Carlos III (ISCIII), the MICIU, and the Pro CNIC Foundation, and is a Severo Ochoa Center of Excellence (CEX2020-001041-S funded by MICIU/AEI/10.13039/501100011033). This publication used the ReDIB ICTS infrastructures at CIC biomaGUNE and CNIC, Ministry for Science and Innovation (MCIN).

### Disclosures

None.

### Supplemental Material

Supplemental Methods
Table S1
Figures S1–S8
Major Resources Table
Statistical Analysis of All Main and Supplemental Figures
Gating Strategy for Flow Cytometry
References 54–59

## REFERENCES

1. Libby P, Buring JE, Badimon L, Hansson GK, Deanfield J, Bittencourt MS, et al. Atherosclerosis. *Nat Rev Dis Prim*. 2019;5:56. doi: 10.1038/s41572-019-0106-z
2. Vallejo J, Cochain C, Zernecke A, Ley K. Heterogeneity of immune cells in human atherosclerosis revealed by scRNA-Seq. *Cardiovasc Res*. 2021;117:2537–2543. doi: 10.1093/cvr/cvab260

3. Roy P, Orecchioni M, Ley K. How the immune system shapes atherosclerosis: roles of innate and adaptive immunity. *Nat Rev Immunol*. 2022;22:251–265. doi: 10.1038/s41577-021-00584-1
4. Wolf D, Ley K. Immunity and inflammation in atherosclerosis. *Circ Res*. 2019;124:315–327. doi: 10.1161/CIRCRESAHA.118.313591
5. Merad M, Sathe P, Helft J, Miller J, Mortha A. The dendritic cell lineage: ontogeny and function of dendritic cells and their subsets in the steady state and the inflamed setting. *Annu Rev Immunol*. 2013;31:563–604. doi: 10.1146/annurev-immunol-020711-074950
6. Cueto FJ, Sancho D. The Flt3l/Flt3 axis in dendritic cell biology and cancer immunotherapy. *Cancers (Basel)*. 2021;13:1525. doi: 10.3390/cancers13071525
7. McKenna HJ, Stocking KL, Miller RE, Brasel K, De Smedt T, Maraskovsky E, Maliszewski CR, Lynch DH, Smith J, Pulendran B, et al. Mice lacking Flt3 ligand have deficient hematopoiesis affecting hematopoietic progenitor cells, dendritic cells, and natural killer cells. *Blood*. 2000;95:3489–3497.
8. Waskow C, Liu K, Darrasse-Jèze G, Guermonprez P, Ginhoux F, Merad M, Shengelia T, Yao K, Nussenzweig M. The receptor tyrosine kinase Flt3 is required for dendritic cell development in peripheral lymphoid tissues. *Nat Immunol*. 2008;9:676–683. doi: 10.1038/ni.1615
9. Sánchez-Paulete AR, Cueto FJ, Martínez-López M, Labiano S, Morales-Kastresana A, Rodríguez-Ruiz ME, Jure-Kunkel M, Azpilikueta A, Aznar MA, Quetglas JI, et al. Cancer immunotherapy with immunomodulatory anti-CD137 and anti–PD-1 monoclonal antibodies requires BATF3-dependent dendritic cells. *Cancer Discov*. 2016;6:71–79. doi: 10.1158/2159-8290.CD-15-0510
10. Murphy TL, Grajales-Reyes GE, Wu X, Tussiwand R, Briseño CG, Iwata A, Kretzer NM, Durai V, Murphy KM. Transcriptional control of dendritic cell development. *Annu Rev Immunol*. 2016;34:93–119. doi: 10.1146/annurev-immunol-032713-120204
11. Dorner BG, Dorner MB, Zhou X, Opitz C, Mora A, Güttler S, Hutloff A, Mages HW, Ranke K, Schaefer M, et al. Selective expression of the chemokine receptor XCR1 on cross-presenting dendritic cells determines cooperation with CD8+ T cells. *Immunity*. 2009;31:823–833. doi: 10.1016/j.immuni.2009.08.027
12. Sancho D, Joffre OP, Keller AM, Rogers NC, Martínez D, Hernanz-Falcón P, Rosewell I, Reis e Sousa C. Identification of a dendritic cell receptor that couples sensing of necrosis to immunity. *Nature*. 2009;458:899–903. doi: 10.1038/nature07750
13. Sancho D, Mourão-Sá D, Joffre OP, Schulz O, Rogers NC, Pennington DJ, Carlyle JR, Reis e Sousa C. Tumor therapy in mice via antigen targeting to a novel, DC-restricted C-type lectin. *J Clin Invest*. 2008;118:2098–2110. doi: 10.1172/JCI34584
14. Henry CM, Castellanos CA, Reis e Sousa C. DNGR-1-mediated cross-presentation of dead cell-associated antigens. *Semin Immunol*. 2023;66:101726. doi: 10.1016/j.smim.2023.101726
15. Bachem A, Güttler S, Hartung E, Ebstein F, Schaefer M, Tannert A, Salama A, Movassaghi K, Opitz C, Mages HW, et al. Superior antigen cross-presentation and XCR1 expression define human CD11c+CD141+ cells as homologues of mouse CD8+ dendritic cells. *J Exp Med*. 2010;207:1273–1281. doi: 10.1084/jem.20100348
16. Ashour D, Arampatzi P, Pavlovic V, Förstner KU, Kaisho T, Beilhack A, Erhard F, Lutz MB. IL-12 from endogenous cDC1, and not vaccine DC, is required for Th1 induction. *JCI Insight*. 2020;5:e135143. doi: 10.1172/jci.insight.135143
17. Zhu J, Paul WE. CD4 T cells: fates, functions, and faults. *Blood*. 2008;112:1557–1569. doi: 10.1182/blood-2008-05-078154
18. Liu TT, Kim S, Desai P, Kim DH, Huang X, Ferris ST, Wu R, Ou F, Egawa T, Van Dyken SJ, et al. Ablation of cDC2 development by triple mutations within the Zeb2 enhancer. *Nature*. 2022;607:142–148. doi: 10.1038/s41586-022-04866-z
19. Mildner A, Jung S. Development and function of dendritic cell subsets. *Immunity*. 2014;40:642–656. doi: 10.1016/j.immuni.2014.04.016
20. Tussiwand R, Everts B, Grajales-Reyes GE, Kretzer NM, Iwata A, Bagaitkar J, Wu X, Wong R, Anderson DA, Murphy TL, et al. Klf4 expression in conventional dendritic cells is required for T helper 2 cell responses. *Immunity*. 2015;42:916–928. doi: 10.1016/j.immuni.2015.04.017
21. Dudziak D, Kamphorst AO, Heidkamp GF, Buchholz VR, Trumpfheller C, Yamazaki S, Cheong C, Liu K, Lee HW, Park CG, et al. Differential antigen processing by dendritic cell subsets in vivo. *Science*. 2007;315:107–111. doi: 10.1126/science.1136080
22. Choi JH, Cheong C, Dandamudi DB, Park CG, Rodriguez A, Mehandru S, Velinzon K, Jung IH, Yoo JY, Oh GT, et al. Flt3 signaling-dependent dendritic cells protect against atherosclerosis. *Immunity*. 2011;35:819–831. doi: 10.1016/j.immuni.2011.09.014
23. Clément M, Haddad Y, Raffort J, Lareyre F, Newland SA, Master L, Harrison J, Ozsvar-Kozma M, Bruneval P, Binder CJ, et al. Deletion of IRF8 (interferon regulatory factor 8)-dependent dendritic cells abrogates proatherogenic adaptive immunity. *Circ Res*. 2018;122:813–820. doi: 10.1161/CIRCRESAHA.118.312713
24. Haddad Y, Lahoute C, Clément M, Laurans L, Metghalchi S, Zeboudj L, Giraud A, Loyer X, Vandestienne M, Wain-Hobson J, et al. The dendritic cell receptor DNGR-1 promotes the development of atherosclerosis in mice. *Circ Res*. 2017;121:234–243. doi: 10.1161/CIRCRESAHA.117.310960
25. Hildner K, Edelson BT, Purtha WE, Diamond M, Matsushita H, Kohyama M, Calderon B, Schraml BU, Unanue ER, Diamond MS, et al. Batf3 deficiency reveals a critical role for CD8alpha+ dendritic cells in cytotoxic T cell immunity. *Science*. 2008;322:1097–1100. doi: 10.1126/science.1164206
26. Li Y, Liu X, Duan W, Tian H, Zhu G, He H, Yao S, Yi S, Song W, Tang H. Batf3-dependent CD8α$^+$ dendritic cells aggravates atherosclerosis via Th1 cell induction and enhanced CCL5 expression in plaque macrophages. *EBioMedicine*. 2017;18:188–198. doi: 10.1016/j.ebiom.2017.04.008
27. Gil-Pulido J, Cochain C, Lippert MA, Schneider N, Butt E, Amézaga N, Zernecke A. Deletion of Batf3-dependent antigen-presenting cells does not affect atherosclerotic lesion formation in mice. *PLoS One*. 2017;12:e0181947. doi: 10.1371/journal.pone.0181947
28. Legein B, Janssen EM, Theelen TL, Gijbels MJ, Walraven J, Klarquist JS, Hennies CM, Wouters K, Seijkens TTP, Wijnands E, et al. Ablation of CD8α$^+$ dendritic cell mediated cross-presentation does not impact atherosclerosis in hyperlipidemic mice. *Sci Rep*. 2015;5:15414. doi: 10.1038/srep15414
29. Liu P, Chen G, Zhang J. A review of liposomes as a drug delivery system: current status of approved products, regulatory environments, and future perspectives. *Molecules*. 2022;27:1372. doi: 10.3390/molecules27041372
30. Zhong H, Chan G, Hu Y, Hu H, Ouyang D. A comprehensive map of FDA-approved pharmaceutical products. *Pharmaceutics*. 2018;10:263. doi: 10.3390/pharmaceutics10040263
31. Zhang J, Zu Y, Dhanasekara CS, Li J, Wu D, Fan Z, Wang S. Detection and treatment of atherosclerosis using nanoparticles. *Wiley Interdiscip Rev Nanomed Nanobiotechnol*. 2017;9:10.1002/wnan.1412. doi: 10.1002/wnan.1412
32. Chen W, Schilperoort M, Cao Y, Shi J, Tabas I, Tao W. Macrophage-targeted nanomedicine for the diagnosis and treatment of atherosclerosis. *Nat Rev Cardiol*. 2022;19:228–249. doi: 10.1038/s41569-021-00629-x
33. Sánchez-Paulete AR, Cueto FJ, Martínez-López M, Labiano S, Morales-Kastresana A, Rodríguez-Ruiz ME, Jure-Kunkel M, Azpilikueta A, Quetglas JI, Sancho D, et al. Cancer immunotherapy with immunomodulatory anti-CD137 and anti-PD-1 monoclonal antibodies requires Batf3-dependent dendritic cells. *Cancer Res*. 2016;76:4908–4908. doi: 10.1158/1538-7445.am2016-4908
34. Durai V, Bagadia P, Granja JM, Satpathy AT, Kulkarni DH, Davidson JT IV, Wu R, Patel SJ, Iwata A, Liu TT, et al. Cryptic activation of an Irf8 enhancer governs cDC1 fate specification. *Nat Immunol*. 2019;20:1161–1173. doi: 10.1038/s41590-019-0450-x
35. Cabeza-Cabrerizo M, Cardoso A, Minutti CM, Pereira Da Costa M, Reis E Sousa C. Dendritic cells revisited. *Annu Rev Immunol*. 2021;39:131–166. doi: 10.1146/annurev-immunol-061020-053707
36. Saigusa R, Winkels H, Ley K. T cell subsets and functions in atherosclerosis. *Nat Rev Cardiol*. 2020;17:387–401. doi: 10.1038/s41569-020-0352-5
37. Hildreth AD, Padilla ET, Gupta M, Wong YY, Sun R, Legala AR, O'Sullivan TE. Adipose cDC1s contribute to obesity-associated inflammation through STING-dependent IL-12 production. *Nat Metab*. 2023;5:2237–2252. doi: 10.1038/s42255-023-00934-4
38. Pham PT, Fukuda D, Nishimoto S, Kim-Kaneyama JR, Lei XF, Takahashi Y, Sato T, Tanaka K, Suto K, Kawabata Y, et al. STING, a cytosolic DNA sensor, plays a critical role in atherogenesis: a link between innate immunity and chronic inflammation caused by lifestyle-related diseases. *Eur Heart J*. 2021;42:4336–4348. doi: 10.1093/eurheartj/ehab249
39. Sauer JD, Sotelo-Troha K, von Moltke J, Monroe KM, Rae CS, Brubaker SW, Hyodo M, Hayakawa Y, Woodward JJ, Portnoy DA, et al. The N-ethyl-N-nitrosourea-induced Goldenticket mouse mutant reveals an essential function of Sting in the in vivo interferon response to Listeria monocytogenes and cyclic dinucleotides. *Infect Immun*. 2011;79:688–694. doi: 10.1128/IAI.00999-10
40. Piemonti L, Monti P, Allavena P, Sironi M, Soldini L, Leone BE, Socci C, Di Carlo V. Glucocorticoids affect human dendritic cell differentiation and maturation. *J Immunol*. 1999;162:6473–6481.

41. Lee W, Kim HS, Hwang SS, Lee GR, The transcription factor Batf3 inhibits the differentiation of regulatory T cells in the periphery. *Exp Mol Med*. 2017;49:e393. doi: 10.1038/emm.2017.157
42. Qiu Z, Khairallah C, Romanov G, Sheridan BS. Batf3 Expression by CD8 T cells critically regulates the development of memory populations. *J Immunol*. 2020;205:901–906. doi: 10.4049/jimmunol.2000228
43. Ataide MA, Komander K, Knöpper K, Peters AE, Wu H, Eickhoff S, Gogishvili T, Weber J, Grafen A, Kallies A, et al. BATF3 programs CD8$^+$ T cell memory. *Nat Immunol*. 2020;21:1397–1407. doi: 10.1038/s41590-020-0786-2
44. Li G, Zhao X, Zheng Z, Zhang H, Wu Y, Shen Y, Chen Q. cGAS-STING pathway mediates activation of dendritic cell sensing of immunogenic tumors. *Cell Mol Life Sci*. 2024;81:149. doi: 10.1007/s00018-024-05191-6
45. Darrasse-Jèze G, Deroubaix S, Mouquet H, Victora GD, Eisenreich T, Yao K, Masilamani RF, Dustin ML, Rudensky A, Liu K, et al. Feedback control of regulatory T cell homeostasis by dendritic cells in vivo. *J Exp Med*. 2009;206:1853–1862. doi: 10.1084/jem.20090746
46. Mor A, Planer D, Luboshits G, Afek A, Metzger S, Chajek-Shaul T, Keren G, George J. Role of naturally occurring CD4+ CD25+ regulatory T cells in experimental atherosclerosis. *Arterioscler Thromb Vasc Biol*. 2007;27:893–900. doi: 10.1161/01.ATV.0000259365.31469.89
47. Ait-Oufella H, Salomon BL, Potteaux S, Robertson AKL, Gourdy P, Zoll J, Merval R, Esposito B, Cohen JL, Fisson S, et al. Natural regulatory T cells control the development of atherosclerosis in mice. *Nat Med*. 2006;12:178–180. doi: 10.1038/nm1343
48. Seillet C, Jackson JT, Markey KA, Brady HJM, Hill GR, Macdonald KPA, Nutt SL, Belz GT. CD8α+ DCs can be induced in the absence of transcription factors Id2, Nfil3, and Batf3. *Blood*. 2013;121:1574–1583. doi: 10.1182/blood-2012-07-445650
49. Tussiwand R, Lee WL, Murphy TL, Mashayekhi M, Wumesh KC, Albring JC, Satpathy AT, Rotondo JA, Edelson BT, Kretzer NM, et al. Compensatory dendritic cell development mediated by BATF-IRF interactions. *Nature*. 2012;490:502–507. doi: 10.1038/nature11531
50. Kim K, Shim D, Lee JS, Zaitsev K, Williams JW, Kim KW, Jang MY, Seok Jang H, Yun TJ, Lee SH, et al. Transcriptome analysis reveals nonfoamy rather than foamy plaque macrophages are proinflammatory in atherosclerotic murine models. *Circ Res*. 2018;123:1127–1142. doi: 10.1161/CIRCRESAHA.118.312804
51. Voloshyna I, Littlefield MJ, Reiss AB. Atherosclerosis and interferon-γ: new insights and therapeutic targets. *Trends Cardiovasc Med*. 2014;24:45–51. doi: 10.1016/j.tcm.2013.06.003
52. Ward NC, Watts GF, Eckel RH. Statin toxicity. *Circ Res*. 2019;124:328–350. doi: 10.1161/CIRCRESAHA.118.312782
53. Engelen SE, Robinson AJB, Zurke YX, Monaco C. Therapeutic strategies targeting inflammation and immunity in atherosclerosis: how to proceed? *Nat Rev Cardiol*. 2022;19:522–542. doi: 10.1038/s41569-021-00668-4
54. Wohn C, Le Guen V, Voluzan O, Fiore F, Henri S, Malissen B. Absence of MHC class II on cDC1 dendritic cells triggers fatal autoimmunity to a cross-presented self-antigen. *Sci Immunol*. 2020;5:eaba1896. doi: 10.1126/sciimmunol.aba1896
55. Voehringer D, Liang HE, Locksley RM. Homeostasis and effector function of lymphopenia-induced "memory-like" T cells in constitutively T cell-depleted mice. *J Immunol*. 2008;180:4742–4753. doi: 10.4049/jimmunol.180.7.4742
56. Song L, Cohen D, Ouyang Z, Cao Y, Hu X, Liu XS. TRUST4: immune repertoire reconstruction from bulk and single-cell RNA-seq data. *Nat Methods*. 2021;18:627–630. doi: 10.1038/s41592-021-01142-2
57. Nazarov V, Tsvetkov V, Fiadziushchanka S, Rumynskiy E, Popov A, Balashov I, et al. Immunarch: bioinformatics analysis of T-cell and B-cell immune repertoires 2023.
58. Zhang H. Thin-film hydration followed by extrusion method for liposome preparation BT. *Methods Mol Biol*. 2017;1522:17–22. doi: 10.1007/978-1-4939-6591-5_2
59. Rouser G, Fkeischer S, Yamamoto A. Two dimensional then layer chromatographic separation of polar lipids and determination of phospholipids by phosphorus analysis of spots. *Lipids*. 1970;5:494–496. doi: 10.1007/BF02531316